

Fall 2-4-2013

Design of a 2.4 GHz Horizontally Polarized Microstrip Patch Antenna using Rectangular and Circular Directors and Reflectors

Yosef Yilak Woldeamanuel

Follow this and additional works at: https://scholarworks.uttyler.edu/ee_grad



Part of the [Electrical and Computer Engineering Commons](#)

Recommended Citation

Woldeamanuel, Yosef Yilak, "Design of a 2.4 GHz Horizontally Polarized Microstrip Patch Antenna using Rectangular and Circular Directors and Reflectors" (2013). *Electrical Engineering Theses*. Paper 14.
<http://hdl.handle.net/10950/104>

This Thesis is brought to you for free and open access by the Electrical Engineering at Scholar Works at UT Tyler. It has been accepted for inclusion in Electrical Engineering Theses by an authorized administrator of Scholar Works at UT Tyler. For more information, please contact tbianchi@uttyler.edu.

DESIGN OF A 2.4GHZ HORIZONTALLY POLARIZED MICROSTRIP
PATCH ANTENNA USING RECTANGULAR AND CIRCULAR
DIRECTORS AND REFLECTORS

by

YOSEF YILAK WOLDEAMANUEL

A thesis submitted in partial fulfillment
of the requirements for the degree of
Master of Science in Electrical Engineering
Department of Electrical Engineering

Hector A. Ochoa, Ph.D., Committee Chair
College of Engineering and Computer Science

The University of Texas at Tyler
November 2012

The University of Texas at Tyler
Tyler, Texas

This is to certify that the Master's Thesis of

YOSEF YILAK WOLDEAMANUEL

has been approved for the thesis requirements on

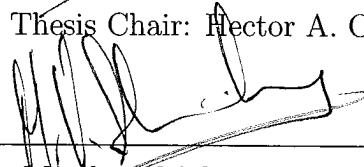
November 7, 2012

for the Master of Science in Electrical Engineering

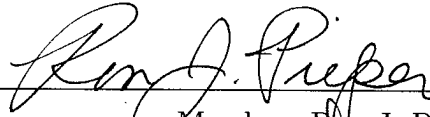
Approvals



Thesis Chair: Hector A. Ochoa, Ph.D.



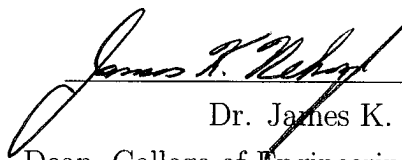
Member: Mukul V. Shirvaikar, Ph.D.



Member: Ron J. Pieper, Ph.D.



Chair and Graduate Coordinator: Mukul V. Shirvaikar, Ph.D.



Dr. James K. Nelson, Jr., Ph.D., P.E.,
Dean, College of Engineering and Computer Science

Acknowledgements

First of all, I would like to give special thanks to my family who has always been there when I needed with constant support and guidance. You never had a doubt in your mind and stood behind me from day one. You always listened and felt my pain. You gave me strength and energy. And you often opened my eyes when I was blind. Thank you so much for just being there! Love you guys!!!!

I would like to thank my advisor, Dr. Hector A. Ochoa, for his continuous encouragement, invaluable supervision, timely suggestions and inspired guidance throughout the completion of this thesis.

I would like to thank Dr. Mukul Shirvaikar for guiding me, advising me and encouraging me throughout my Master's program. I would like to thank my committee member Dr. Ron J. Pieper for taking time and reviewing my work. I also would like to thank the entire EE department faculty members for their support and encouragement they gave to me.

Finally, I extend my gratitude to one and all who are directly or indirectly involved in the successful completion of this thesis work.

Table of Contents

List of Tables	iv
List of Figures	v
Abstract	vii
Chapter One: Background	1
1.1 Introduction	1
1.2 Types of Antennas	1
1.2.1 Wire Antennas	1
1.2.2 Aperture Antennas	2
1.2.3 Microstrip Antennas	2
1.2.4 Array Antennas	3
1.2.5 Reflector Antennas	4
1.2.6 Lens Antennas	4
1.3 Fundamental Parameters of Antenna	5
1.3.1 Radiation Pattern	5
1.3.2 BeamWidth	6
1.3.3 Radiation Intensity	7
1.3.4 Directivity	8
1.3.5 Antenna Efficiency	8
1.3.6 Antenna Gain	9

1.3.7	BandWidth	9
1.3.8	Polarization	10
1.3.9	Input Impedance	10
1.4	Antenna Modeling	12
1.5	Antenna Simulation Software	14
Chapter Two:	Microstrip Antenna	16
2.1	Introduction	16
2.2	Radiation Mechanism of Microstrip Antenna	18
2.3	Feeding Techniques and Modeling	19
2.4	Microstrip Antenna Design Considerations	20
2.4.1	Substrate Selection	20
2.4.2	Element Width and Length	21
2.4.3	Radiation Patterns and Radiation Resistance	23
2.4.4	Feed Point Location	24
2.4.5	Polarization	25
Chapter Three:	Microstrip Patch Antenna Design and Simulation Results	26
3.1	Review of Relevant Works	26
3.2	Microstrip Patch Antenna Design	27
3.3	Simulation Results	29
3.3.1	Radiation Pattern	29
3.3.2	Antenna Gain	31
3.3.3	Return Loss	32
3.4	Directors and Reflectors Design	32
3.5	Design 1 : Rectangular Reflector and Four Rectangular Directors	34
3.5.1	Radiation Pattern	35

3.5.2	Antenna Gain	36
3.5.3	Return Loss	37
3.6	Design 2 : Loop Director and Rectangular Reflector	41
3.6.1	Radiation Pattern	42
3.6.2	Antenna Gain	43
3.6.3	Return Loss	44
Chapter Four:	Conclusion and Future Work	48
4.1	Conclusion	48
4.2	Future Work	49
References	50

List of Tables

Table 3.1	Antenna Elements Dimensions,Locations, and Substrate Thickness	35
Table 3.2	Antenna Elements Dimensions,Locations, and Substrate Thickness	41
Table 3.3	Antenna Elements Dimensions,Locations, and Substrate Thickness	45

List of Figures

Figure 1.1	Wire antenna configuration	2
Figure 1.2	Aperture antenna configurations	3
Figure 1.3	Rectangular microstrip patch antenna	3
Figure 1.4	Array configurations(Yagi Uda and Microstrip Array)	4
Figure 1.5	Reflector antenna configuration	5
Figure 1.6	Lens antenna configurations	5
Figure 1.7	Coordinate system for antenna analysis	6
Figure 1.8	Radiation lobes and beam widths of an antenna pattern	7
Figure 1.9	Polarizations (Linear, Circular, and Elliptical)	11
Figure 1.10	Geometry of Yee cell	14
Figure 2.1	Microstrip patch antenna configuration	17
Figure 2.2	Microstrip antenna charge distribution and current density	18
Figure 2.3	Fringing fields for the dominant mode in a rectangular Microstrip patch	19
Figure 2.4	Magnetic and electric wall model of microstrip patch antenna	21
Figure 2.5	Two slots model	22
Figure 3.1	Rectangular microstrip patch antenna configuration	28
Figure 3.2	2D ($\phi=0$ degrees) cut view of E- field	30
Figure 3.3	3D far zone total E-Field distribution	30
Figure 3.4	3D far zone E-Field distribution (Theta view)	31

Figure 3.5	3D far zone E-Field distribution (Phi view)	31
Figure 3.6	2D (phi=0 degrees) cut view of the gain	33
Figure 3.7	3D far zone total gain	33
Figure 3.8	Return loss (S11) and steady state parameters	34
Figure 3.9	Microstrip antenna configuration with Directors and Reflector . .	35
Figure 3.10	2D (phi=0 degrees) cut view of E- field	36
Figure 3.11	3D far zone total E-Field distribution	36
Figure 3.12	Radiation pattern variation with director positions	37
Figure 3.13	2D (phi=0 degrees) cut view of the gain	38
Figure 3.14	3D far zone total gain	38
Figure 3.15	Return loss (S11) and steady state parameters	39
Figure 3.16	Microstrip patch antenna configuration with directors and reflector	39
Figure 3.17	3D far zone total gain	40
Figure 3.18	Microstrip patch antenna configuration with loop director	41
Figure 3.19	2D (phi=0 degrees) cut view of E- field	42
Figure 3.20	3D far zone total E-Field distribution	42
Figure 3.21	2D (phi=0 degrees) cut view of the gain	43
Figure 3.22	3D far zone total gain	43
Figure 3.23	Return loss (S11) and steady state parameters	44
Figure 3.24	Microstrip antenna configuration with three reflectors	45
Figure 3.25	2D (phi=0 degrees) cut view of the gain	46
Figure 3.26	3D far zone total gain	46
Figure 3.27	Return loss (S11) and steady state parameters	47

Abstract

DESIGN OF A 2.4GHZ HORIZONTALLY POLARIZED MICROSTRIP PATCH ANTENNA USING RECTANGULAR AND CIRCULAR DIRECTORS AND REFLECTORS

YOSEF YILAK WOLDEAMANUEL

Thesis Chair: Hector A. Ochoa, Ph.D.

The University of Texas at Tyler

November 2012

In the urban or indoor wireless environment, after a complicated multiple reflection or scattering effect, the polarization of the propagating radio wave may change significantly. Although many current wireless systems are vertically polarized, it has been predicted that it is advantageous to use horizontally polarized antennas at both the transmitter and receiver ends. A horizontally polarized antenna is less likely to pick up man-made interference produced by automobile ignition systems and electrical appliances, which is usually vertically polarized. A second advantage is that there is less absorption of radiated energy by buildings or wiring when these antennas are used. Another advantage is that support structures for these antennas are of a more convenient size than those for vertically polarized antennas. Finally, horizontally polarized waves suffer lower losses than vertically polarized waves, especially above 100 MHz.

Modern communication systems and instruments such as Wireless Local Area Networks (WLAN), mobile handsets and local positioning systems (LPS) require lightweight, small size and low cost antennas. The selection of microstrip antenna technology can fulfill these requirements. The main problem is that they usually radiate in a direction along the ground plane (vertically), and the gain in the horizontal direction is

only a few decibels.

In this thesis, new designs are proposed to develop a horizontally polarized microstrip patch antennas for 2.4 GHz applications using directors and reflectors to guide the radiated power. This thesis will focus on the development of designs which retain the advantages of microstrip patch antenna while improving its horizontal radiation. The results from the two most significant antenna configurations are discussed and analyzed. The first design is composed of four rectangular directors and one rectangular reflector. The second design is composed of one loop director and one rectangular reflector. The radiation characteristics of these designs with respect to various geometrical parameters such as the dimensions of the reflector and directors, and spacing between these elements are studied in order to obtain the best possible performance. Furthermore, two-dimensional and three-dimensional radiation patterns, antenna gain and return loss for each of these designs are presented.

The results from the first design yielded a radiation pattern with an elevation of 20 degrees with a maximum gain of 2.033 dBi. The proposed antenna structure has dimensions of 61.785mm x 67.65 mm, and a total height of 35.794mm. The results from the second design yielded a radiation pattern with an elevation of 0 degrees with a maximum gain of 3.847 dBi. The compactness of the overall antenna structure was further improved to 61.875mm x 67.65mm, and a total height of 30.794mm. The input impedance and resonance center frequencies are also in the desired range for both designs. The proposed compact antennas present an excellent candidate for the emerging wireless communications with large amount of data transmitting in rapid bursts requirement at 2.4 GHz frequency, which include Bluetooth and WiFi (802.11).

Chapter One

Background

1.1 Introduction

An antenna is a device used to transform an RF signal, traveling on a conductor, into an electromagnetic guided wave in free space, and vice versa (i.e., in either transmitting or receiving mode of operation). Antennas are frequency-dependent devices. Each antenna is designed for a certain frequency band, and it rejects signals beyond the operating band. For that reason, antennas can be considered bandpass filters and transducers. In addition, an antenna in advanced wireless systems is usually required to optimize or accentuate the radiation energy in some directions and suppress it in others. Nowadays, these devices constitute an essential part of wireless communication systems [1].

Basic antenna classification depends on design particularities, mode of operations and their applications. The isotropic point source radiator, which radiates the same intensity of electromagnetic signal in all directions, is considered as a benchmark for other antennas. However, these sources do not exist, but most antennas' gains are measured with respect to this specific radiator.

1.2 Types of Antennas

1.2.1 Wire Antennas

Wire antennas are a simple and familiar type of antenna, which are seen almost everywhere - on automobiles, buildings, ships, and aircraft. There are various shapes of wire antennas such as a straight wire (dipole), loop, and helix. In the case of loop antennas, they are not required to possess a circular shape. They can take the form of a rectangle, square, ellipse, or any other desired shape. However, the circular loop

is the most common configuration, because of its simplicity in construction. The configuration of the dipole and circular loop antenna is shown in figure 1.1.



Figure 1.1: Wire antenna configuration

1.2.2 Aperture Antennas

The use of aperture antennas is becoming more and more typical. An aperture antenna contains some sort of opening through which electromagnetic waves are transmitted or received. Examples of aperture antennas include slots, waveguides, and horn antennas. Three different configurations of horn antennas (pyramidal, conical, and rectangular) are shown in the figure 1.2. Antennas of this type are very useful in space missions, because they can be used to produce wide-beam coverage and can be conveniently flush-mounted onto the skin of the aircraft or spacecraft. In addition, they can be covered with a dielectric material to protect them from hazardous conditions.

1.2.3 Microstrip Antennas

Microstrip antennas became very popular in the 1970s primarily for spaceborne applications. Today, they are heavily used for government and commercial applications. These antennas consist of a metallic patch on a grounded substrate. A graphical representation of a microstrip patch antenna is shown in figure 1.3. The metallic patch

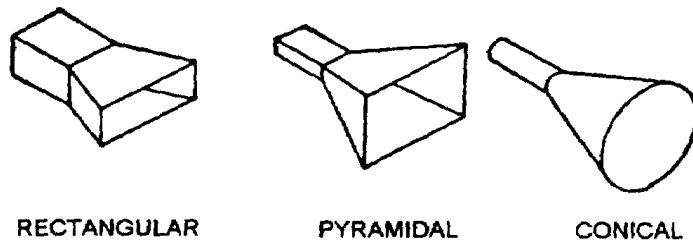


Figure 1.2: Aperture antenna configurations

on the top of the substrate can take different configurations. However, the rectangular and circular patches are the most popular, because they are easy to analyze and fabricate, and their attractive radiation characteristics, especially low cross-polarization radiation. Microstrip antennas have low profile, and they are simple and inexpensive to fabricate using modern printed-circuit technology. They are also mechanically robust when mounted on rigid surfaces, and compatible with Monolithic Microwave Integrated Circuit (MMIC) designs. Microstrip antennas are versatile in terms of resonant frequency, polarization, radiation pattern, and impedance. These antennas can be mounted on the surface of high-performance aircraft, spacecraft, satellites, missiles, cars, and even handheld mobile devices [2].

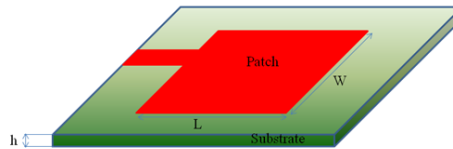


Figure 1.3: Rectangular microstrip patch antenna

1.2.4 Array Antennas

Many applications require radiation patterns and gains that may not be achieved by a single element antenna. In order to obtain the desired radiation characteristics

several single antenna elements are combined to form an antenna array. Examples of a microstrip patch array and a Yagi - Uda array are shown in figure 1.4. The arrangement of the array is in such a way that the radiation from each individual element adds up to produce a maximum radiation in a particular direction or directions. The overall radiation characteristics of array antennas can be influenced by the number of elements, spacing, and radiating element properties. Unlike a single element antenna whose radiation pattern is fixed, the radiation pattern of array antennas, called the array pattern, can be changed upon exciting its elements with different currents. This provides a freedom to design a certain desired array pattern from an array without changing its physical dimensions [3].

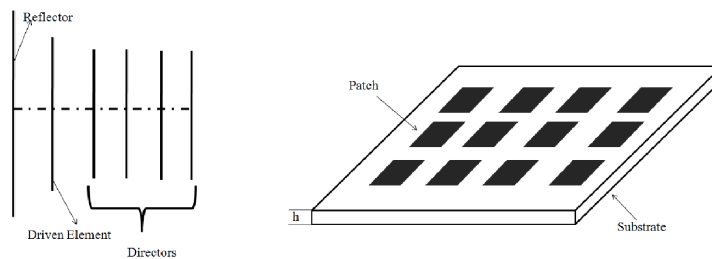


Figure 1.4: Array configurations(Yagi Uda and Microstrip Array)

1.2.5 Reflector Antennas

Reflector antennas are high gain antennas, which can easily achieve gains above 30 dB for microwave and higher frequencies. They are used for long distance radio communication, high-resolution radars, and radio-astronomy. A typical example of a reflector antenna configuration is the parabolic reflector shown in figure 1.5. Antennas of this type have been built with diameters as large as 305 m [4].

1.2.6 Lens Antennas

Lenses are primarily used to collimate incident divergent energy to prevent it from spreading in undesired directions. By properly shaping the geometrical configuration and choosing the appropriate material of the lenses, they can transform various forms

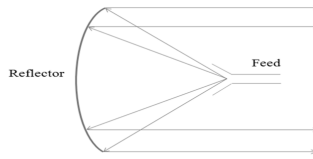


Figure 1.5: Reflector antenna configuration

of divergent energy into plane waves. They can be used in most of the applications in which the parabolic reflectors are implemented, especially at higher frequencies. One major disadvantage of these antennas is that their dimensions and weight become exceedingly large at low frequencies. Lens antennas are classified according to the material from which they are constructed, or according to their geometrical shape. A convex-plane and concave-plane lens antenna configurations are shown in figure 1.6.



Figure 1.6: Lens antenna configurations

1.3 Fundamental Parameters of Antenna

1.3.1 Radiation Pattern

An antenna radiation pattern or antenna pattern is defined as a mathematical function or a graphical representation of how the electric or magnetic field intensities vary with respect to the angular positions, elevation and azimuth, for a fixed range. Radiation properties include power flux density, radiation intensity, field strength, directivity, phase or polarization. In most cases, the radiation pattern is determined in the far field region and is represented as a function of the directional coordinates. The far field region is the region farthest away from the antenna where the field dis-

tribution is independent of the distance from the antenna. It is identified by those distances greater than $2D^2/\lambda_o$, D being the maximum overall dimension of the antenna and λ_o the free-space wavelength [5].

In general, most of the radiation patterns are composed of multiple lobes, which may

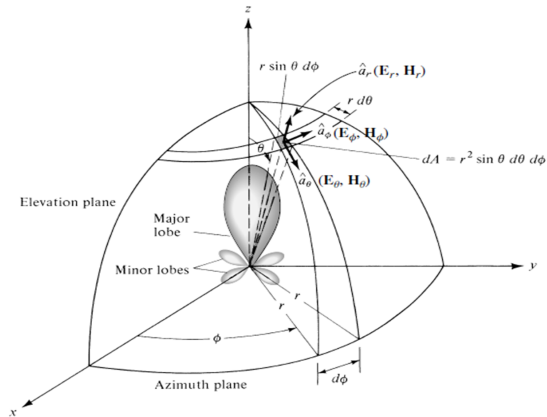


Figure 1.7: Coordinate system for antenna analysis

be sub classified into major or main, minor, side, and back lobes as shown in figure 1.7. A radiation lobe is a portion of the radiation pattern bounded by regions of relatively weak radiation intensity. A major lobe (also called main beam) is defined as the radiation lobe containing the direction of maximum radiation. In some antennas, such as split-beam antennas, there may exist more than one major lobe. A sidelobe is a radiation lobe in any direction other than the intended lobe. Usually a sidelobe is adjacent to the main lobe and occupies the hemisphere in the direction of the main beam. A backlobe is a radiation lobe whose axis makes an angle of approximately 180° with respect to the beam of an antenna. Usually it refers to a minor lobe that occupies the hemisphere in a direction opposite to that of the major (main) lobe [1].

1.3.2 BeamWidth

The beamwidth of an antenna is defined as the angular separation between two identical points on opposite sides of the pattern maximum. In an antenna pattern, there are a number of beamwidths as indicated in figure 1.8. One of the most widely used beamwidth is the Half-Power Beamwidth (HPBW), which is defined by IEEE as, "In a plane containing the direction of the maximum of a beam, the angle between

the two directions in which the radiation intensity is one-half value of the beam” [4]. Another important beamwidth is the angular separation between the first nulls of the pattern, and it is referred to as the First-Null Beam width (FNBW). Other beamwidths are those where the pattern is -10 dB from the maximum, or any other value. However, in practice, the term beamwidth, with no other identification, usually refers to HPBW [1]. The beamwidth of an antenna is an important parameter, and often is used to describe the resolution capabilities of the antenna to distinguish between two adjacent radiating sources or radar targets.

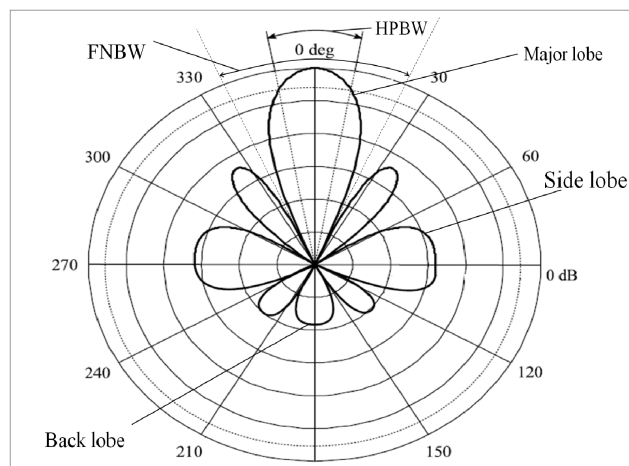


Figure 1.8: Radiation lobes and beam widths of an antenna pattern

1.3.3 Radiation Intensity

Radiation intensity in a given direction is defined as the power radiated from an antenna per unit solid angle. The radiation intensity is a far-field parameter, and it can be obtained by multiplying the radiation density by the square of the distance. In a mathematical form, it is expressed as

$$U = r^2 W_{rad} \quad (1.1)$$

Where

U - radiation intensity (W/unit solid angle)

W_{rad} - radiation density (W/m^2)

r - distance (m)

1.3.4 Directivity

The Directivity of an antenna is defined as the ratio of the radiation intensity in a given direction from the antenna to the radiation intensity averaged over all directions. The average radiation intensity is equal to the total power radiated by the antenna divided by 4π . If the direction is not specified, the direction of maximum radiation intensity is implied. The directivity of a non isotropic source is equal to the ratio of its radiation intensity in a given direction over that of an isotropic source. In a mathematical form, it can be written as

$$D = \frac{U}{U_o} = \frac{4\pi U}{P_{rad}} \quad (1.2)$$

Where

D = directivity (dimensionless)

U = radiation intensity (W/unit solid angle)

U_o = radiation intensity of isotropic source (W/unit solid angle)

Many times it is desirable to express the directivity in decibels (dB) instead of dimensionless quantities. The expressions for converting the dimensionless quantities of directivity and maximum directivity to decibels (dB) is $D(\text{dB}) = 10 \log_{10}[D(\text{dimensionless})]$

1.3.5 Antenna Efficiency

Related with an antenna, there are a number of efficiencies. The total efficiency, takes into account losses at the input terminals and with the structure of the antenna. Such losses may be due to reflections because of the mismatch between the transmission line and the antenna, and I^2R losses (conduction and dielectric). The overall efficiency can be written as

$$e_o = e_r e_c e_d \quad (1.3)$$

Where

e_o = total efficiency (dimensionless)

e_r = reflection (mismatch) efficiency = $(1 - |\Gamma|^2)$ (dimensionless)

e_c = conduction efficiency (dimensionless)

e_d = dielectric efficiency (dimensionless)

Γ = voltage reflection coefficient at the input terminals of the antenna

$\Gamma = (Z_{in} - Z_o)/(Z_{in} + Z_o)$ where Z_{in} = antenna input impedance, Z_o = characteristic impedance of the transmission line.

$$VSWR = VoltageStandingWaveRatio = \frac{1 + |\Gamma|}{1 - |\Gamma|} \quad (1.4)$$

1.3.6 Antenna Gain

Another useful measure describing the performance of an antenna is the gain. Although the gain of the antenna is closely related to the directivity, it is a measure that takes into account the efficiency of the antenna as well as its directional capabilities. It is defined as the ratio of the intensity, in a given direction, to the radiation intensity that would be obtained if the power accepted by the antenna were radiated isotropically. The radiation intensity corresponding to the isotropically radiated power is equal to the power accepted (input) by the antenna divided by 4π

$$Gain = 4\pi \frac{RadiationIntensity}{TotalPower} = 4\pi \frac{U(\theta, \phi)}{P_{in}} \quad (1.5)$$

In most cases, the gain is relative, which is defined as the ratio of the power gain in a given direction to the power gain of a reference antenna in its referenced direction. The reference antenna is usually a dipole or isotropic antenna [6].

1.3.7 BandWidth

The bandwidth of an antenna is defined as the range of frequencies within which the performance of the antenna, with respect to some characteristic, conforms to a specified standard. The bandwidth can be considered to be the range of frequencies, on either side of a center frequency, usually the resonance frequency. In this range, the antenna characteristics such as input impedance, pattern, beamwidth, polarization, side lobe level, gain, and radiation efficiency are within an acceptable value of those at the center frequency. For broadband antennas, the bandwidth is usually expressed as the ratio of the upper-to-lower frequencies of acceptable operation. For example, a 10:1 bandwidth indicates the upper frequency is 10 times greater than the lower. For narrowband antennas, the bandwidth is expressed as a percentage of the frequency

difference (upper minus lower) over the center frequency of the bandwidth. For example, a 5 percent bandwidth indicates that the frequency difference of acceptable operation is 5 percent of the center frequency of the bandwidth [1].

1.3.8 Polarization

Polarization of a radiated wave is defined as the property of an electromagnetic wave describing the time-varying direction and relative magnitude of the electric-field vector. It is described by the geometric figure traced by the electric field vector upon a stationary plane perpendicular to the direction of propagation, as the wave travels through that plane. The three different types of antenna polarizations are shown in figure 1.9. Vertical, and horizontal polarizations are the simplest forms of antenna polarization and they both fall into a category known as linear polarization. It is also possible that antennas can have a circular polarization. Circular polarization occurs when two or more linearly polarized waves add together, such that the E-field of the net wave rotates. Circular polarization has a number of benefits for areas such as satellite applications where it helps overcome the effects of propagation anomalies, ground reflections and the effects of the spin that occur on many satellites [7]. Another form of polarization is known as elliptical polarization. It occurs when there is a mix of linear and circular polarization. This can be visualized by the tip of the electric field vector tracing out an elliptically shaped corkscrew. It is possible for linearly polarized antennas to receive circularly polarized signals and vice versa. But, there is a 3 dB polarization mismatch between linearly and circularly polarized antennas [8].

1.3.9 Input Impedance

Antenna impedance is presented as the ratio of voltage to current at the antenna's terminals. In order to achieve maximum energy transfer the input impedance of the antenna must identically match the characteristic impedance of the transmission line. If the two impedances do not match, a reflected wave will be generated at the antenna terminal and travel back towards the energy source. This reflection of energy results in a reduction in the overall antenna efficiency. The impedance of an antenna, with no load attached, is defined as:

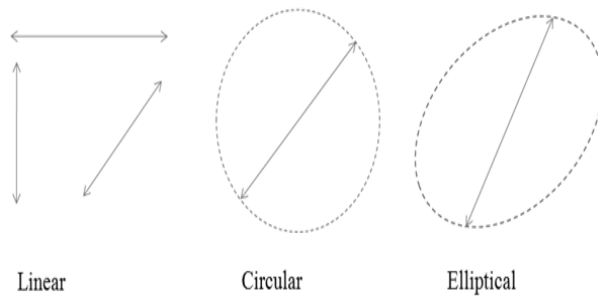


Figure 1.9: Polarizations (Linear, Circular, and Elliptical)

$$Z_A = R_A + jX_A \quad (1.6)$$

Where

Z_A = antenna impedance (ohms)

R_A = antenna resistance (ohms)

X_A = antenna reactance (ohms)

The resistive part

$$R_A = R_r + R_L \quad (1.7)$$

Where

R_r = radiation resistance of the antenna

R_L = loss resistance of the antenna

The input impedance of an antenna is generally a function of frequency. Thus, the antenna will be matched to the interconnecting transmission line and other associated equipment only within a bandwidth. In addition, the input impedance of the antenna depends on many factors including its geometry, its method of excitation, and its proximity to surrounding objects. Because of their complex geometries, only a limited number of practical antennas had been investigated analytically. For many others, the input impedance has been determined experimentally.

1.4 Antenna Modeling

Maxwell's partial differential equations of electrodynamics were formulated around 1870. It has been considered as the most outstanding achievement of the 19th-century science. Maxwell's equations represent a fundamental unification of electric and magnetic fields predicting electromagnetic wave phenomena. The solution of Maxwell's equations is an area of significant importance to the microwave and antenna engineering community [4].

$$\begin{aligned}\nabla \times E &= -\frac{\partial B}{\partial t} \\ \nabla \times H &= J + \frac{\partial D}{\partial t} \\ \nabla \cdot D &= \rho \\ \nabla \cdot B &= 0\end{aligned}\tag{1.8}$$

Maxwell's equations are usually solved by one of three different techniques, namely, mathematical analysis, experimental observation or numerical simulation. In the past, engineers and researchers from all around the world have used computers ranging from simple desktop machines up to massive parallel supercomputing arrays to obtain solutions to these equations for the purpose of investigating electromagnetic wave guiding, radiation and scattering problems. With the ever fast development of modern computer technology, existing computational electromagnetic (CEM) techniques have become more and more popular and have been applied to problems ranging from basic antenna analysis to complex biological interaction issues. As well as the increase in popularity of existing methods, the new computer technology has also opened up other opportunities for the development of new techniques for CEM. In general, the techniques used in CEM can be divided into two major categories: numerical methods and high-frequency or asymptotic methods. The numerical methods are classified either as differential-equation-based or integral-equation-based. Both categories can be divided into two classifications, frequency domain and time domain. There are various time domain and frequency domain techniques, two well-known examples are the Finite Difference Time Domain (FDTD) method and Method of Moments (MoM). The FDTD technique uses a set of iterative equations to solve Maxwell's equations in differential form in the time domain via a time marching scheme. This method is physically straightforward and mathematically simple; as a result, it has become very popular. On the other hand, Finite Difference Time Domain (FDTD) seeks a direct solution for Maxwell's time-dependent curl equations [9].

$$\begin{aligned}\sigma \vec{E} + \varepsilon \frac{\partial \vec{E}}{\partial t} &= \nabla \times \vec{H} \\ \mu \frac{\partial \vec{H}}{\partial t} &= -\nabla \times \vec{E}\end{aligned}\tag{1.9}$$

Instead of employing potentials to find solution for the Maxwell curl equations, The FDTD is based upon volumetric sampling of the unknown near field distribution within and surrounding the structure of interest over a finite period of time. In this approach, the space is divided into discrete cells, which should be small compared to the wavelength. The electric fields are located on the edges of the box, and the magnetic fields are positioned on the faces as shown in figure 1.10. This orientation of the fields is known as the Yee cell and is the basis for FDTD [9]. Time is quantized into small steps where each step represents the time required for the field to travel from one cell to the next. The electric and magnetic fields are updated using a leapfrog scheme where first the electric fields, then the magnetic are computed at each step in time. When many FDTD cells are combined together to form a three-dimensional volume, the result is an FDTD grid or mesh. Each FDTD cell will overlap edges and faces with its neighbors, by convention each cell will have three electric fields that begin at a common node associated with it. The electric fields at the other nine edges of the FDTD cell will belong to other adjacent cells. Each cell will also have three magnetic fields originating on the faces of the cell adjacent to the common node of the electric fields [2].

The FDTD is a general method since it aims at solving Maxwell's partial differential equations directly without analytical preprocessing and modeling. Therefore, complex antennas can also be analyzed using this technique. Some of the advantages of the FDTD techniques are:

- From a mathematical point of view it is a direct implementation of Maxwell's curl equations. Therefore, analytical processing of Maxwell's equations is almost negligible.
- It is capable of predicting broadband frequency response because, the analysis is carried out in the time domain.
- It is capable of analyzing complex systems, including wave interaction with human body, or satellite, nonlinear device simulation, and complex antennas.

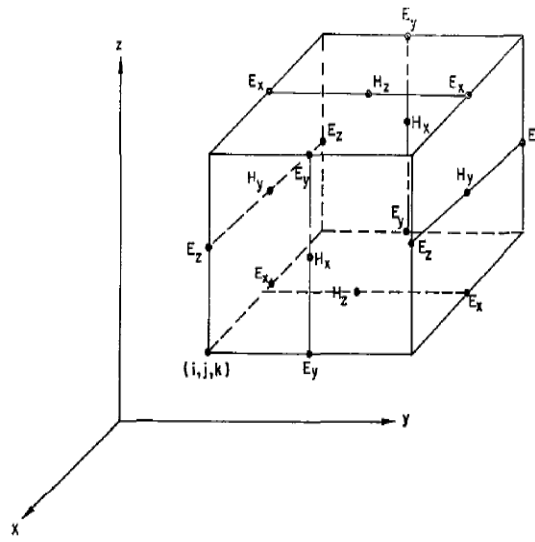


Figure 1.10: Geometry of Yee cell

- It is capable of analyzing structures using different types of materials, for example, lossy dielectrics, magnetized ferrites, and anisotropic plasmas.
- It provides a real-time animation display, which is a powerful tool for both a student and an electromagnetic designer [2].

1.5 Antenna Simulation Software

Although many techniques for accurately simulating the electromagnetic characteristics of antennas exist, it is difficult to design a good antenna system. Antennas are frequently designed through an ad-hoc combination of experience, intuition, and guesswork [7]. Designing antennas for multiple frequency ranges and diverse applications is even more complicated. There exists a need for new technologies and methodologies to supplement traditional antenna design techniques. Electromagnetic Professional (EMPro), is Agilent EEsof EDA's EM simulation software design platform for analyzing 3D electromagnetic (EM) effects of components such as high-speed and RF IC packages, bondwires, antennas, on-chip and off-chip embedded passives and PCB interconnects. EMPro EM simulation software features a modern design, simulation and analysis environment, high capacity simulation technologies and in-

tegration with the industry's leading RF and microwave circuit design environment, Advanced Design System (ADS) for fast and efficient RF and microwave circuit design.

Key Benefits of EMPro EM Simulation Software

- **Design Flow Integration:** Create 3D components that can be simulated together with 2D circuit layouts and schematics within Advanced Design System (ADS), using EM-circuit cosimulation.
- **Broad Simulation Technology:** Set up and run analyses using both frequency-domain and time-domain 3D EM simulation technologies: Finite Element Method (FEM) and Finite Difference Time Domain (FDTD).
- **Efficient User Interface:** Quickly create arbitrary 3D structures with a modern, simple GUI that saves time and EMPro EM simulation software provides advanced scripting features [10].

Chapter Two

Microstrip Antenna

2.1 Introduction

The concept of Microstrip radiators was first proposed by Georges A. Deschamps in 1953. However, 20 years passed before practical antennas were actually fabricated. The development of these antennas during the 1970s was accelerated by the availability of good substrate with low loss tangent and attractive thermal and mechanical properties. Also, the improvement in photolithographic techniques and the availability of suitable theoretical models helped the fast development of these antennas. The first practical antennas were developed by Howell and Munson in the early 1970's [2]. Microstrip antennas have considerably matured in the last 25 years, and many of their limitations have been overcome.

Microstrip antennas are low profile, light weight, inexpensive and easy to integrate with accompanying electronics antennas. They are most suitable for aerospace and mobile applications. Many of the antenna applications for satellite links, mobile communications, and wireless local-area networks, impose constraints on compactness, dual frequency operation, frequency agility, polarization control, and radiation control. These functions can be achieved by properly loading a simple Microstrip antenna. For that reason, they are becoming more and more popular [6]. The characteristics of microstrip antennas can be significantly improved by using multilayered structures with thick substrate and low permittivity materials. Because of their low power handling capabilities, these antennas can also be used in low power transmitting and receiving applications.

As shown in figure 2.1, a Microstrip antenna in its simplest configuration consists of a radiating patch on one side of a dielectric substrate which has a ground plane on the other side. The patch conductors normally made of copper or gold, can assume

virtually any shape, but regular shapes, such as rectangles and circles, are generally used to simplify performance prediction. Ideally, the dielectric constant ϵ_r , of the substrate should be low ($\epsilon_r < 2.5$), to enhance the fringing fields that account for radiation [2].

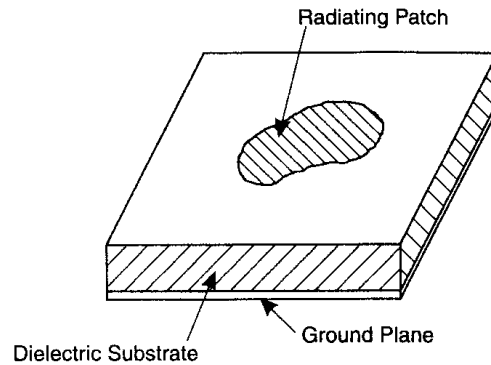


Figure 2.1: Microstrip patch antenna configuration

Microstrip antennas have several advantages compared to conventional antennas. Many applications that cover a frequency range of 100 MHz to 100GHz use these structures. Some of the principal advantages of Microstrip antennas are:

- Light weight, low volume, and thin profile configuration;
- Low fabrication cost;
- Linear and circular polarizations are possible with simple feed;
- Dual frequency and dual polarization antennas can be easily made;
- Can be easily integrated with microwave integrated circuits;
- Feed lines and matching networks can be fabricated with antenna structures.

However, Microstrip antennas also have some limitations compared to conventional antennas:

- Narrow bandwidth and tolerance problems;
- Somewhat lower gain;
- Large ohmic loss in the feed structures and arrays;
- Complex feed structures are required for high performance arrays;
- High cross polarizations and mutual coupling at high frequencies.

2.2 Radiation Mechanism of Microstrip Antenna

The important characteristic of Microstrip antennas is their inherent ability to radiate efficiently despite their low profile. The primary source of radiation is the electric fringing fields between the edges of the conductor element and the ground plane. Thick substrates with low permittivity are used in Microstrip antennas for better radiation efficiency [11]. The radiation from Microstrip antenna can be determined from the field distribution between the patch metallization and the ground plane. Alternatively, radiation can be described in terms of the surface current distribution. An accurate calculation of the field or current distribution of the patch antenna is complicated. However, crude approximations and simple arguments can be used to develop a workable model for Microstrip antennas. A patch, which is connected to a microwave source, has a charge distribution on the upper and lower surface of the patch as well as the ground plane as shown in figure 2.2. The excitation of the patch results in positive and negative charge distribution, mainly because the patch is half wavelength in the dominant mode [12].

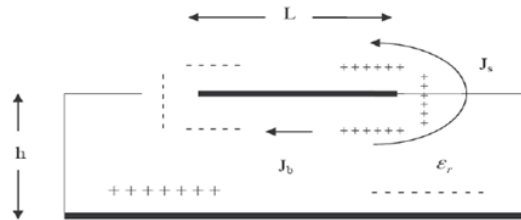


Figure 2.2: Microstrip antenna charge distribution and current density

The repulsive nature of those charges at the bottom surface of the patch pushes some

charges around the side to the top generating the current densities J_b and J_s . In microstrip antennas, the height to width ratio (h/W) is small as compared to the overall patch length. Therefore, the strong attractive forces between the charges cause that most of the current and charge concentration remains underneath the patch. However, also the repulsive force between positive charges creates a large charge density around the edges. The fringing fields generated by these charges are responsible for the radiation. Figure 2.3 shows the fringing fields in a Microstrip patch.

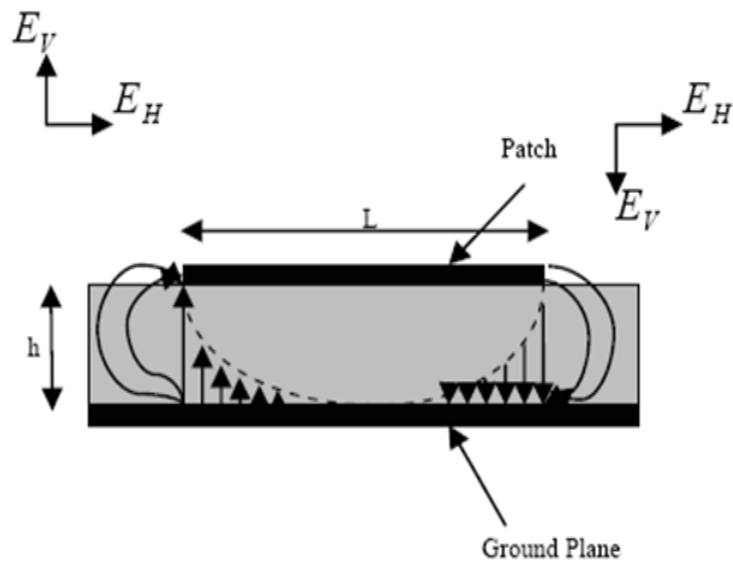


Figure 2.3: Fringing fields for the dominant mode in a rectangular Microstrip patch

2.3 Feeding Techniques and Modeling

Microstrip antennas have radiating elements on one side of the dielectric substrate. Thus, early microstrip antennas were fed either by a microstrip-line or a coaxial probe through the ground plane. The selection of feeding techniques is governed by a number of factors. The most important consideration is the efficient power transfer between the radiating structure and the feed structure, that is, impedance matching between the radiating and the feed structures. Microstrip patch antennas can be fed by a variety of methods. These methods can be classified into two categories-

contacting and non-contacting. In the contacting method, the RF power is fed directly to the radiating patch using a connecting element such as a microstrip-line. In the non-contacting scheme, electromagnetic field coupling is done to transfer power between the microstrip-line and the radiating patch. The four most popular feeding techniques are the microstrip-line, coaxial probe (both contacting schemes), aperture coupling and proximity coupling (both non-contacting schemes). Excitation of microstrip antennas by a microstrip-line on the same substrate appears to be a natural choice, because the patch can be considered an extension of the microstrip-line, and both can be fabricated simultaneously.

The simple transmission line model, the generalized transmission line model, and the cavity model are some of the techniques used to analyze patch antennas. These models are used to predict the characteristics of a microstrip patch antenna. These include its resonant frequency, bandwidth, radiation pattern, etc. The cavity model becomes a natural choice to analyze microstrip antennas due to the fact that microstrip patch antennas are narrow-band resonant antennas, which can be termed lossy cavities. In this model, the interior region of the patch is modeled as a cavity bounded by electric walls on the top and bottom, and a magnetic wall all along the periphery. The bases for this assumption are,

- The fields in the interior region do not vary with z (that is, $\partial/\partial z \equiv 0$), because the substrate is very thin, ($h \ll \lambda_o$).
- The electric field is radiated only in the z -direction, and the magnetic field has only the transverse components in the region bounded by the patch metallization and the ground plane.
- The electric current in the patch has no component normal to the edge of the patch metallization, which implies that the tangential component (y and z directions) of H along the edge is negligible, and a magnetic wall can be placed along the periphery ($\partial E_z/\partial n \equiv 0$).

2.4 Microstrip Antenna Design Considerations

2.4.1 Substrate Selection

It is critical for the design of these antennas to select a suitable dielectric substrate of appropriate thickness h , and loss tangent. A thicker substrate, besides being me-

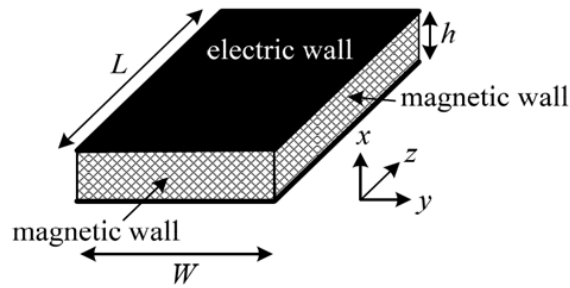


Figure 2.4: Magnetic and electric wall model of microstrip patch antenna

mechanically strong, will increase the radiated power, reduce conductor loss and improve impedance bandwidth. However, it will also increase the weight, dielectric loss, surface wave loss and extraneous radiation from the probe feed. A rectangular patch antenna stops resonating for a substrate thickness greater than $0.11\lambda_o$ due to inductive reactance of the feed. The substrate dielectric constant (ϵ_r) plays a role similar to that of substrate thickness. A low dielectric constant for the substrate will increase the fringing field at the patch periphery. As a result, the radiated power of the antenna will be also increased. Therefore, a dielectric constant of less than 2.55 ($\epsilon_r < 2.55$) is preferred unless a smaller patch size is desired. An increase in the substrate thickness has similar effects on the antenna characteristics as decreasing the value of the dielectric constant. A high substrate loss tangent increases the dielectric loss of the antenna and reduces the antenna efficiency. The most commonly used substrate materials are honeycomb ($\epsilon_r=1.07$), duroid ($\epsilon_r=2.32$), Quartz ($\epsilon_r=3.8$), and alumina ($\epsilon_r=10$).

2.4.2 Element Width and Length

Patch width has a minor effect on the resonant frequency and radiation pattern of the antenna. However, it affects the input resistance and bandwidth to a larger extent. A bigger patch width increases the power radiated and thus provides a decreased resonant resistance, increased bandwidth, and increased radiation efficiency. A constraint against a larger patch width is the generation of grating lobes in antenna arrays. It has been suggested that the length to width ratio of the path has to lie in the range of one and two ($1 < L/W < 2$) to obtain a good radiation efficiency. The patch length

determines the resonant frequency, and is a critical parameter in the design, because of the inherent narrow bandwidth of the patch. The microstrip patch length (L), for TM₁₀ (Transverse Magnetic) mode of operation can be approximated as;

$$L = \frac{c}{2f_r\sqrt{\epsilon_r}} \quad (2.1)$$

Where

c - Speed of light in free space

f_r - Resonant frequency

ϵ_r - Dielectric constant of the substrate

In practice, the fields are not confined to the patch. A fraction of the fields lie outside the physical dimensions of the patch ($L \times W$) as shown in figure 2.5. This is called the fringing field.

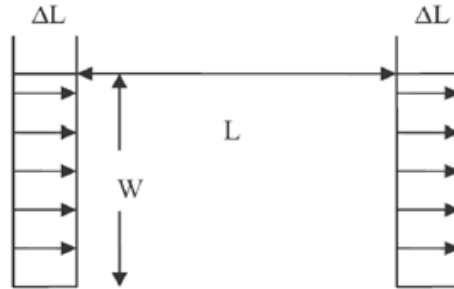


Figure 2.5: Two slots model

The effect of the fringing field along the patch width, W can be included through the effective dielectric constant ϵ_{eff} for a Microstrip line of width W on the given substrate [13].

$$\epsilon_{eff} = \frac{\epsilon_r + 1}{2} + \frac{\epsilon_r - 1}{2} \left(1 + 12 \frac{h}{W}\right)^{-\frac{1}{2}} \quad (2.2)$$

Where

ε_{eff} = Effective dielectric constant
 ε_r = Dielectric constant of substrate
 h = Height of dielectric substrate
 W = Width of the patch

Whereas the effect of the fringing field along the patch length L can be described in terms of an additional line length on either ends of the patch length.

$$\Delta L = \frac{0.41h(\varepsilon_{eff} + 0.3)\left(\frac{W}{h}\right) + 0.264}{(\varepsilon_{eff} - 0.258)\left(\frac{W}{h} + 08\right)} \quad (2.3)$$

The effective length is given by:

$$L_{eff} = L + 2\Delta L \quad (2.4)$$

The resonant frequency is:

$$f_r = \frac{c}{2L_{eff}\sqrt{\varepsilon_{eff}}} \quad (2.5)$$

2.4.3 Radiation Patterns and Radiation Resistance

The radiation patterns of microstrip antennas are of prime importance in determining most of its radiation characteristics, which include beam-width, beam shape, side-lobe level, directivity, polarization and radiated power. Radiation from a patch can be derived either from the E_z field across the aperture between the patch and the ground plane (using vector electric potential) or from the currents on the surface of the patch conductor (employing vector magnetic potentials). The two-slot model and electric surface current model are commonly used to calculate the radiation patterns of microstrip antennas. In the first case, the antenna is modeled as a combination of two parallel slots of length W , width h , and spaced a distance L apart, whereas in the second case, the patch metallization is replaced by the surface current distribution. The radiation patterns obtained from the two different approaches are very similar.

The directivity is a measure of the directional properties of a microstrip antenna compared to those of an isotropic antenna. The directivity is always greater than unity since an isotropic radiator is not directional. The directivity is defined as the ratio of maximum power density in the main beam direction to the average radiated power density. A simple approximate expression for the directivity D of a rectangular patch is given as

$$D \approx \frac{4(k_o W)^2}{\Pi \eta_o G_r} \quad (2.6)$$

where $\eta_o = 120\Pi\Omega$, G_r = radiation conductance of the patch. The directive gain G of the antenna is defined as

$$G = e_r D \quad (2.7)$$

Where e_r is the radiation efficiency of the antenna. This efficiency is defined as the ratio of the radiated power (P_r) to the input power (P_i). The input power is transformed into radiated power and surface wave power while a small portion is dissipated due to conductor and dielectric losses of the materials used. Antenna gain can also be specified using the total efficiency instead of using only radiation efficiency. This total efficiency is a combination of the radiation efficiency and efficiency linked to the impedance matching of the antenna. The gain is always less than directivity because e_r lies in the range of zero and one ($0 < \epsilon_r < 1$).

Another important parameter of antennas is the bandwidth. Most of the times, the impedance bandwidth is mentioned in antennas specification. However, it is important to realize that several definitions of bandwidth exist; impedance bandwidth, directivity bandwidth, polarization bandwidth, and efficiency bandwidth. Directivity and efficiency are often combined as gain bandwidth.

2.4.4 Feed Point Location

After selecting the patch dimensions L and W for the given substrate, the feed point has to be determined to achieve a good impedance match between the generator impedance and input impedance of the patch element. The change in feed location gives rise to a change in the input impedance and hence provides a simple method for

impedance matching. The feed point is selected such that the input resistance R_{in} is equal to the feed line impedance, usually taken to be 50Ω .

2.4.5 Polarization

The polarization of a rectangular patch antenna is linear and directed along the resonating dimension, when operated in the dominant mode. Large bandwidth patch antennas may operate in the higher order mode also. The radiation pattern and polarization for these modes can be different from the dominant mode. Another source for cross-polarization is the fringing field along the non-radiating edges. These fields are oriented 90 degrees with respect to the field at the radiating edges. Their contribution to the radiation fields in the E and H planes is zero. However, in the intercardinal planes, even the ideal, single mode patch will radiate cross-polarized fields. The cross-polarization level increases with substrate thickness. Polarization of the antenna can be changed mechanically or electronically. For the electronic tuning, PIN diodes or varactor diodes can be used [2]. Polarization diversity is used in mobile communications to account for the reduction in signal strength due to fading.

Chapter Three

Microstrip Patch Antenna Design and Simulation Results

This chapter will discuss the procedures used to design the configurations of the proposed microstrip patch antenna. Also, in this chapter, the radiation characteristics for each of the designs will be discussed.

3.1 Review of Relevant Works

The approaching maturity of microstrip antenna technology coupled with the increasing demand and applications for such devices has resulted in a huge volume of research work in the field of microstrip antennas. The most relevant publications for this specific research include "Vertically Multilayer-stacked Yagi antenna with Single and Dual polarizations" by Olivier Kramer, Tarek Djerafi, and Ke Wu [14], and "Microstrip Yagi Array Antenna for Mobile Satellite Vehicle Application" by John Huang, and Athur C. Densmore [15].

In the first paper, high gain and compact stacked multilayered Yagi antennas were proposed and demonstrated at 5.8 GHz for a local positioning system. The proposed structure was made of vertically stacked Yagi like parasitic director elements to obtain a high antenna gain. Two different antenna configurations were proposed. The first one based on a dipole geometry for single polarization and the second one on a circular patch to achieve dual polarization. The result from this research work presents a very directive and symmetric radiation pattern.

The work also suggests that the proposed designs provide a number of advantages compared to uni-planar Yagi antennas. First, the usage of a third dimension (the vertical dimension) that has not been widely used in the design of microstrip antennas, allows an effective reduction in size, and footprint. Second, a high permittivity

substrate can be used, reducing spacing between the directors, which is critical for a high-density integration between antenna and circuits. Third, wide bandwidth characteristics can be achieved by implementing dual polarization designs based on the Yagi antenna concept, and coupling-based feed mechanisms. Finally, the design of such antennas over millimeter-wave and terahertz ranges where the substrate spacing between Yagi antenna elements can naturally be made compatible with current three-dimensional circuit processing techniques.

In the work done by Huang and Densmore, a very low profile and medium gain antenna for satellite vehicle application was proposed. The design contained an antenna active patch (driven element) and a parasitic patch (reflector and director elements) located on the same horizontal plane. They suggested that in order for microstrip patches to function similarly to the standard Yagi array antenna, the adjacent patches need to be placed closely to each other so that a significant amount of coupling can be obtained through surface waves in the substrate. They also proposed the dimension ratio between the director patch and the driven element patch to be between 0.8 and 0.95; The distance between the centers of the reflector and the driven elements to be about 0.35 free-space wavelengths, while the separation between the centers of the director and driven elements to be approximately 0.3 free-space wavelength.

3.2 Microstrip Patch Antenna Design

Based on the microstrip patch antenna design considerations mentioned in section 2.4, Duroid 5870/5880 was chosen as the dielectric substrate for the antenna. This material is lightweight, and possesses a low dielectric constant ($\epsilon_r = 2.33$). It also has uniform electrical properties over a wide frequency range. In order to achieve a high radiation power without increasing the antenna weight and the dielectric loss, a 1.575 mm thick substrate is selected from the available commercial duroid substrate [16]. As show in the figure 3.1 a patch length (L) of 41mm and width (W) of 37.5mm are calculated using equations 2.1-2.7 for a resonant frequency of 2.4GHz. The feed position must be located at a point on the patch where the input impedance is 50 ohms for the resonant frequency. The equations used to calculate the exact feed position are very complex. However, by using equation 3.1 an initial estimate of the feed location can be calculated [17].

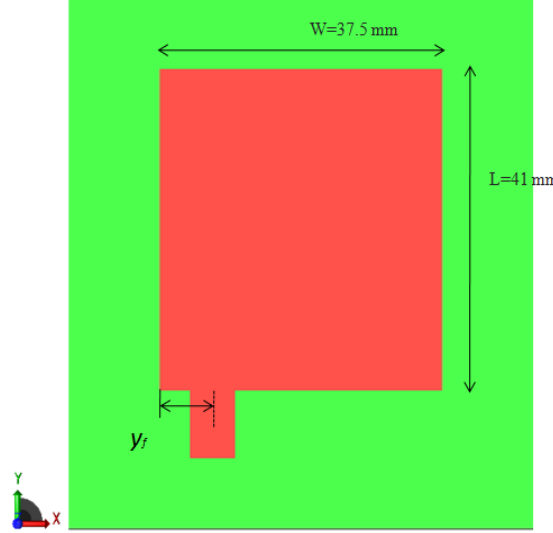


Figure 3.1: Rectangular microstrip patch antenna configuration

$$R_{in} \approx \frac{R_r}{2} [1 - \sin(\frac{\Pi}{L} \cdot y_f)] \quad (3.1)$$

Where

R_{in} - Input resistance

y_f - Position of feed from patch edge

L - Patch Length

R_r - Radiating resistance (for $W < \lambda_0$, $R_r = 90 \cdot \frac{(\lambda_0)^2}{W^2}$)

As a result, an approximate of 14.5mm is calculated for y_f , which will be optimized by the simulation software to achieve a 50 ohms antenna input impedance.

Typically, the size of the ground plane is assumed to be infinite during the analysis and design of microstrip patch antennas. In an actual application only a finite size ground plane can be implemented. The implementation of a finite ground plane induces diffraction of radiation from the edges of the ground plane, resulting in a change in radiation pattern, radiation conductance, and resonant frequency. But, if the size of the ground plane is greater than the patch dimensions by approximately six times the substrate thickness all around the periphery, a similar radiation char-

acteristic for finite and infinite ground plane can be obtained [2].

3.3 Simulation Results

As explained in section 1.4, using the FDTD method to model an antenna has many advantages. Such as, direct implementation of Maxwell's curl equations, capability of predicting broadband frequency response, analyzing structures using different types of materials, and provides a real-time animation display. There is available different commercial antenna simulation software that uses FDTD method. EMPro is a three dimensional full wave electromagnetic solver that uses FDTD and Finite Element method (FEM) to run analyses both in the frequency domain and in the time domain. Besides the available FDTD method, EMPro has a parameterization feature that can be used to optimize the design to achieve better radiation characteristics.

The simulation results of the designed rectangular patch antenna radiation characteristics (radiation pattern, antenna gain and return loss) using EMPro 3D simulation software are presented in the following sections.

3.3.1 Radiation Pattern

In order to compare the change in radiation characteristics for the proposed designs, the radiation characteristics for a regular microstrip patch antenna are presented. Figures 3.2 - 3.5 present the simulated 2D cut view and 3D far zone E-plane radiation patterns for this antenna. These results show that the microstrip patch antenna mainly radiates in the vertical direction. This is in agreement with the theoretical radiation pattern for these structures. It is also observed that the radiation pattern possess a high directivity and symmetry [2][18].

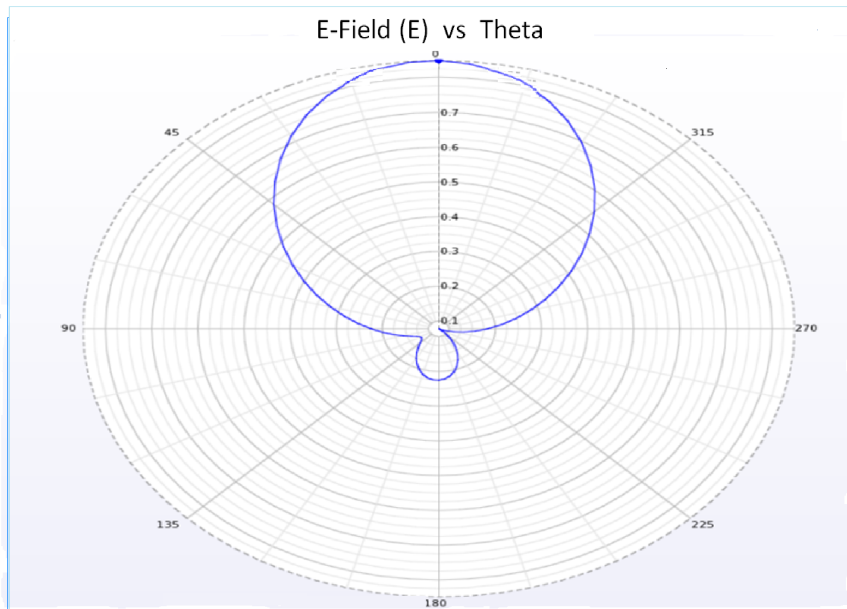


Figure 3.2: 2D ($\phi=0$ degrees) cut view of E- field

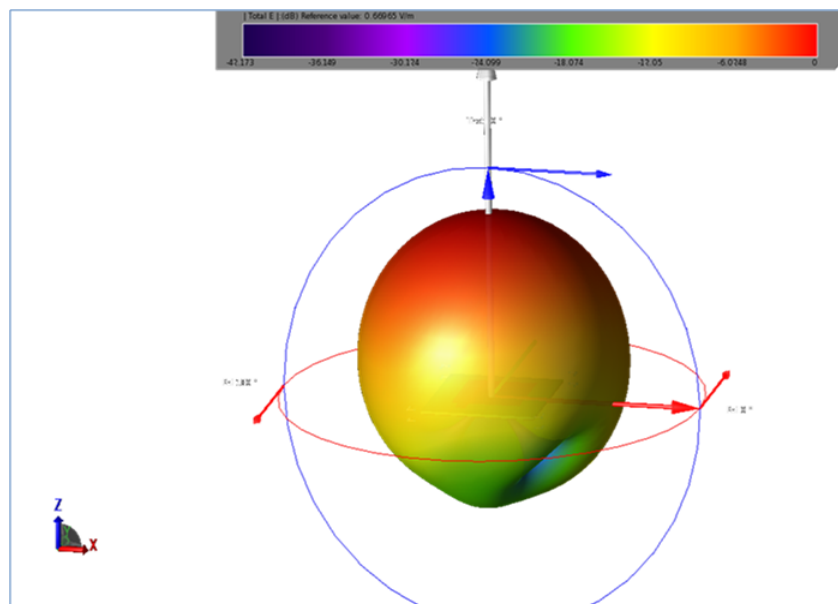


Figure 3.3: 3D far zone total E-Field distribution

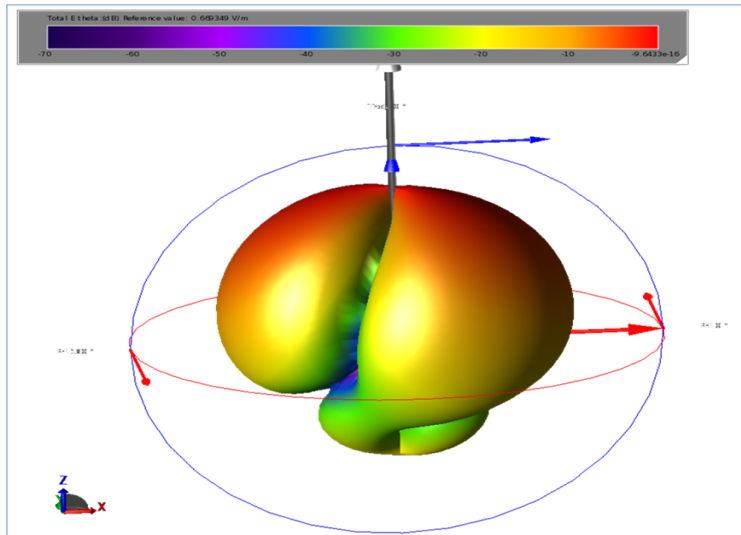


Figure 3.4: 3D far zone E-Field distribution (Theta view)

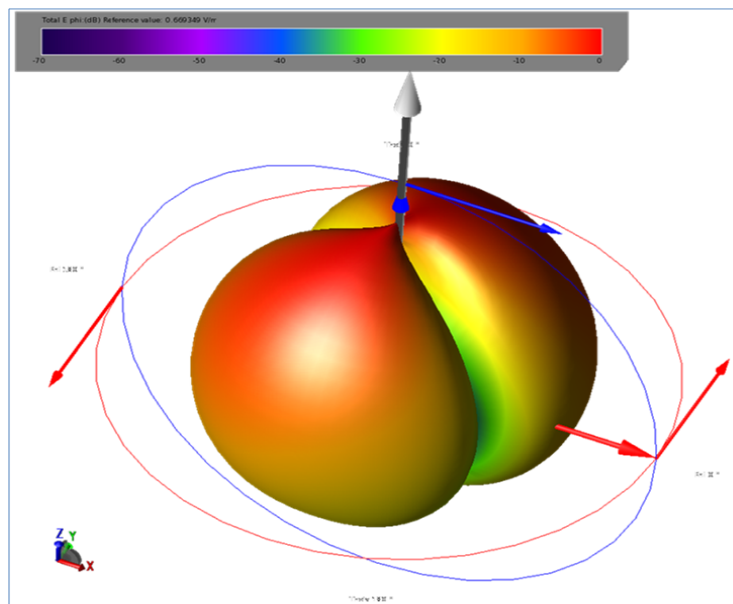


Figure 3.5: 3D far zone E-Field distribution (Phi view)

3.3.2 Antenna Gain

As shown in figures 3.6 and 3.7 a maximum antenna gain of 7.083dBi with a main lobe in the direction of $\theta = 0$ degrees and $\phi = 0$ degrees was obtained. The

simulated gain is a little higher compared to the results reported by Bhartia, Bahl, and Garg [2].

3.3.3 Return Loss

The simulated S-parameter versus frequency and the steady state parameters in the time domain at 2.4GHz are presented in figure 3.8. It can be seen that the simulated center frequency is slightly shifted from the designed target, but still very close to 2.4GHz, and an input impedance of 48.718 Ohms is obtained, which is fairly close to the standard 50 Ohms antenna input impedance.

3.4 Directors and Reflectors Design

The design of a microstrip Yagi antenna implements a similar principle as conventional Yagi-Uda dipole array, where the electromagnetic energy is coupled from the driven element dipole through space into the parasitic dipoles and then reradiated to form a directional beam. In a microstrip Yagi array, the electromagnetic energy is coupled from the driven patch to the parasitic patches not only through space, but also by surface waves in the substrate. Unlike a dipole antenna, the microstrip patch radiates primarily in its broadside direction. As a consequence, the adjacent patches need to be placed close to each other ($0.15\lambda_0$ to $0.2\lambda_0$) in order to function similar to Yagi dipoles [15].

The parasitic elements of the microstrip Yagi antenna operate by re-radiating their energy in a slightly different phase to that of the driven element which reinforce the driven element signal in some directions and cancel out in others. The amplitude and phase of the induced current depend on the separation between the parasitic elements and the driver element. Also, the length of the parasitic elements affects the induced current. In order to obtain the required phase shift the parasitic element can be made either inductive or capacitive. If the parasitic element is made inductive, the induced currents are in such a phase that they reflect the power away from the parasitic element. This causes the microstrip patch antenna to radiate more power away from it. These types of elements are known as reflectors. In order to make these elements inductive their resonant length should be longer compared to the patch length. If the parasitic element is made capacitive, the induced currents are in such a phase that

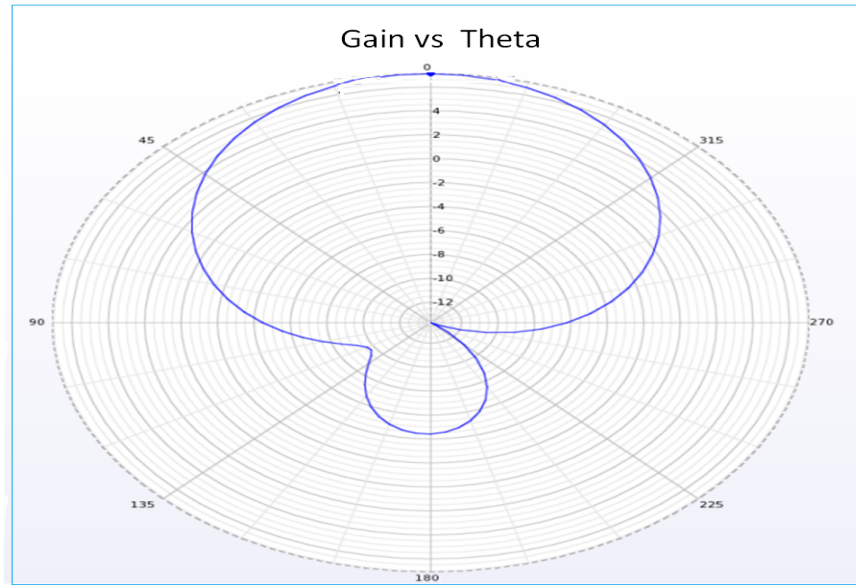


Figure 3.6: 2D ($\phi=0$ degrees) cut view of the gain

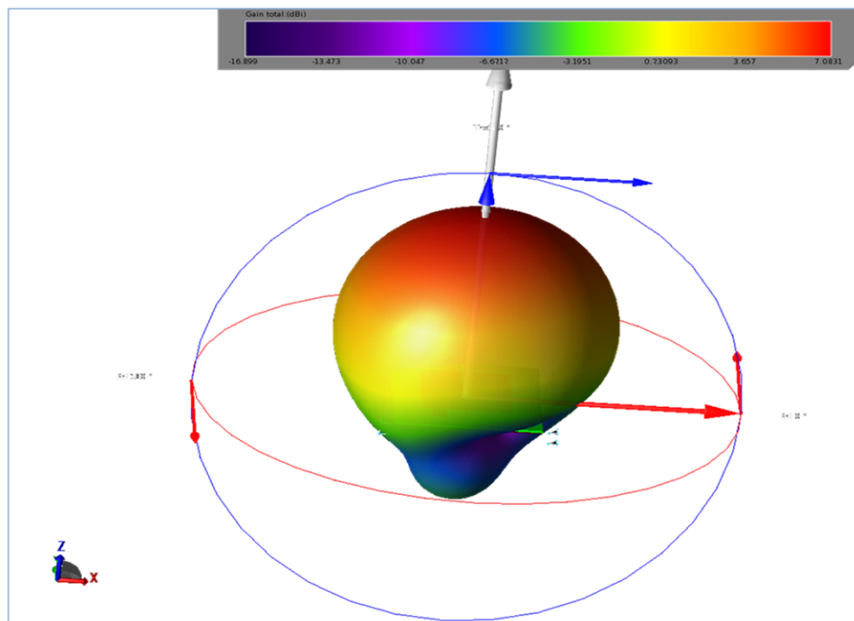


Figure 3.7: 3D far zone total gain

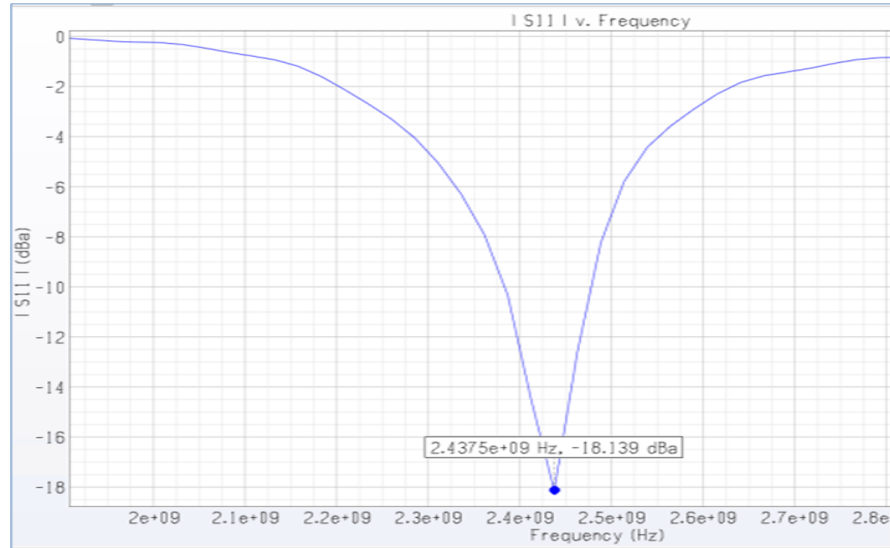


Figure 3.8: Return loss (S11) and steady state parameters

they direct the power radiated by the whole antenna in the direction of the parasitic element. These types of elements are known as directors [14][15].

In the following sections, the results from the two most significant designs will be discussed and analyzed. It needs to be noted that more designs were studied, but their results were not good enough to be included in this document.

3.5 Design 1 : Rectangular Reflector and Four Rectangular Directors

The configuration of the proposed microstrip patch antenna is composed by four directors and one reflector as shown in figure 3.9. The same substrate used for the microstrip patch is used to support the directors and reflector on the top of the patch. In order to reduce the overall weight of the design, the thickness of the substrate for the directors and the reflector is chosen to be 0.794mm. The entire size of the designed structure is optimized as shown in table 3.1 in order to achieve a horizontal radiation with the highest possible gain.

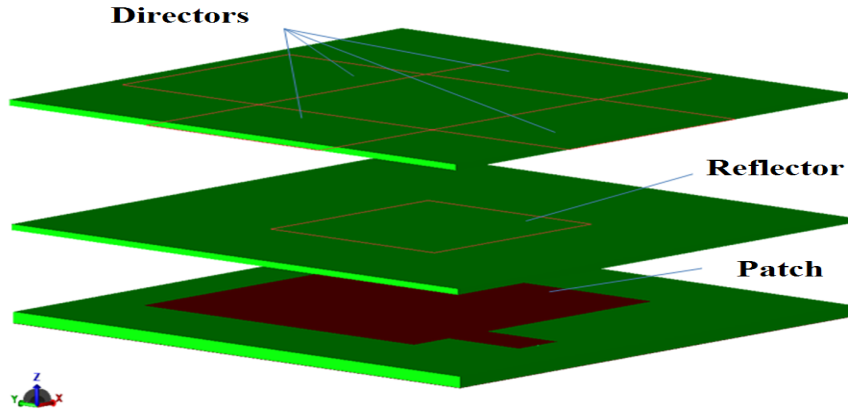


Figure 3.9: Microstrip antenna configuration with Directors and Reflector

Directors				Reflector			
Length	Width	Location	Substrate (h)	Length	Width	Location	Substrate (h)
26.25 mm	17.8 mm	35 mm	0.794 mm	29.25 mm	29.25 mm	12.75 mm	0.794 mm
Total height = 35mm + 0.794mm = 35.794mm Dimension = 61.875mm x 67.65mm x 35.794mm							

Table 3.1: Antenna Elements Dimensions, Locations, and Substrate Thickness

3.5.1 Radiation Pattern

Figures 3.10 and 3.11 show the simulated radiation pattern (2D cut view and 3D far zone) when design 1 is considered. It can be seen that the E-plane radiation pattern is mainly radiating in the horizontal direction. For this specific case the main lobe is located at $\theta=70$ degrees and $\Phi=175$ degrees (20 degrees elevation). It can also be seen that the radiation pattern for this design possesses a back lobe. However, this is not of big importance because it is small compared to the main lobe.

The radiation pattern in the horizontal directions ($\theta = 90$ degrees and $\theta = 270$ degrees) can be improved by moving the directors closer to the microstrip patch as shown in the figure 3.12. But at the same time the radiation in the vertical direction ($\theta = 180$ degrees) is increased which causes a decrease in the overall antenna gain.

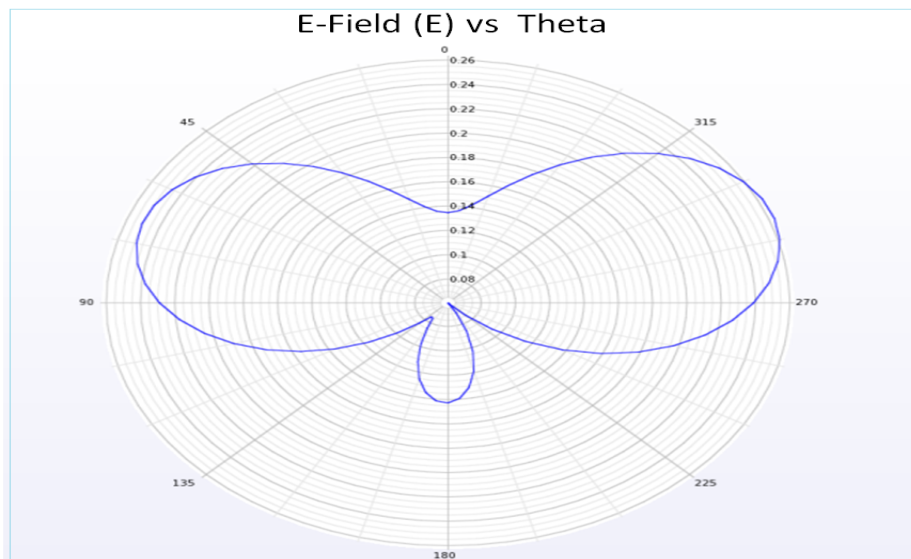


Figure 3.10: 2D ($\phi=0$ degrees) cut view of E- field

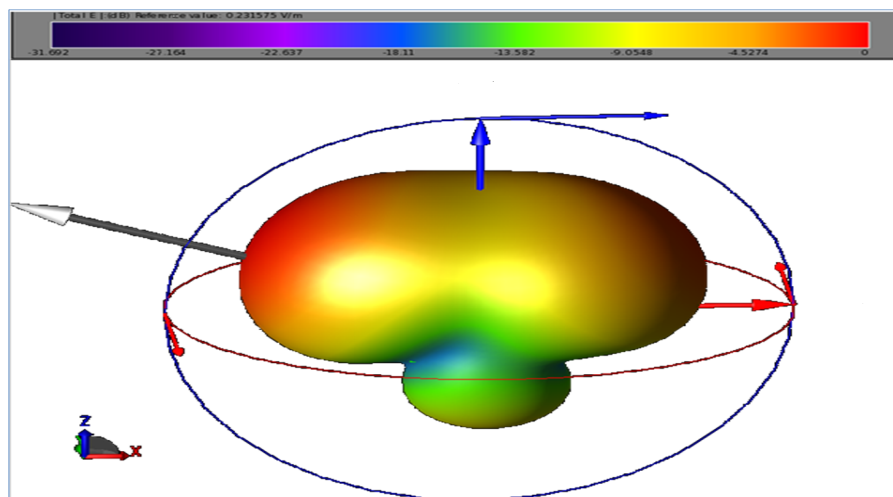


Figure 3.11: 3D far zone total E-Field distribution

3.5.2 Antenna Gain

In figures 3.13 and 3.14 it can be seen the 2D and 3D far zone overall antenna gain for Design 1. After optimizing the position and size of the directors and reflector a maximum gain of 1.33dBi was obtained. The reason for the gain being low compared

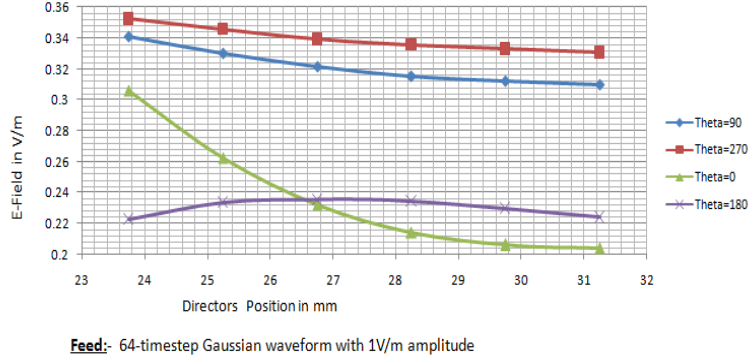


Figure 3.12: Radiation pattern variation with director positions

to the rectangular patch antenna is that the microstrip patch antenna covers a wide solid angle which makes it best suited for applications that require a wide coverage in short distances.

As reported in [2][19], although most horizontally polarized antennas have a low gain, it has been predicted that using horizontally polarized antenna at both the transmitter and receiver will result in 10dB more power as compared to the power received using vertically polarized antennas at both end of the link. The reason is that horizontally polarized antennas are less likely to pick up manmade interference, which is normally vertically polarized. When antennas are located near dense forests, horizontally polarized waves suffer smaller losses compared to vertically polarized waves, especially above 100MHz. Small changes in antenna location do not cause large variations in the field intensity of horizontally polarized waves when an antenna is located among trees or buildings. When vertical polarization is used, a change of only a few feet in the antenna location may have a significant effect on the received signal strength [20].

3.5.3 Return Loss

The S11-parameter (return loss) versus frequency and time domain steady state parameters at 2.4GHz are presented in figure 3.15. It is observed that the center resonant

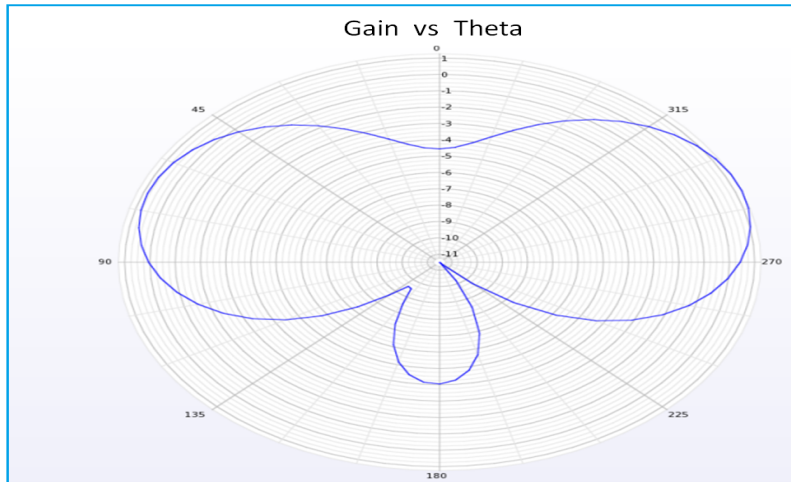


Figure 3.13: 2D ($\phi=0$ degrees) cut view of the gain

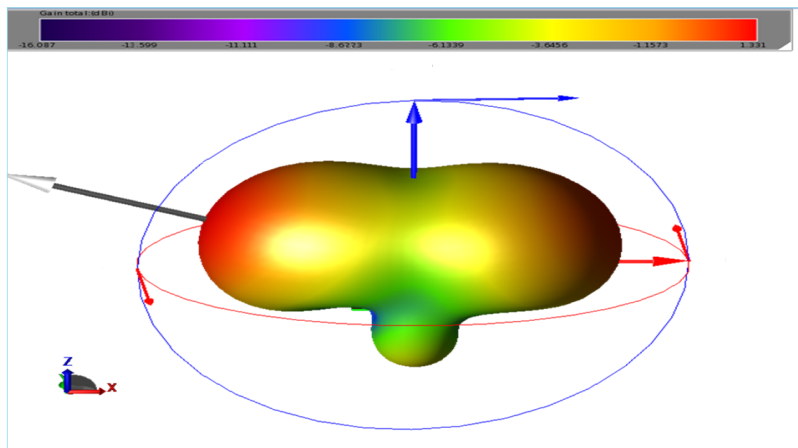


Figure 3.14: 3D far zone total gain

frequency has been shifted to a lower frequency due to the reactance variation of the antenna due to the reflector and directors. The input impedance of the antenna has also decreased to 41.734 Ohms, and it has become more reactive.

A better microstrip patch antenna gain of 2.033 dBi is obtained by removing the extension of the substrate beyond the dimensions of reflector and directors except for

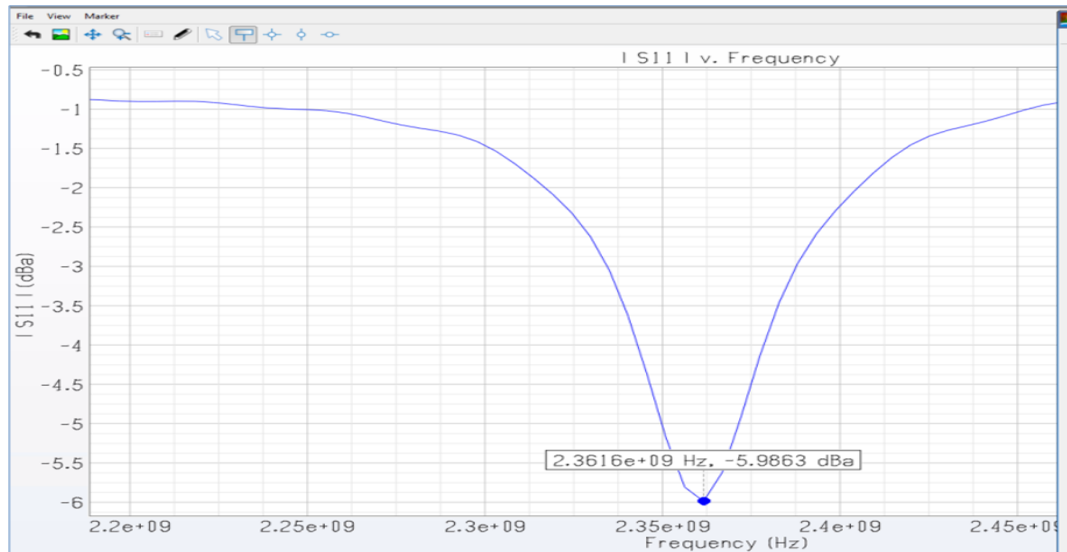


Figure 3.15: Return loss (S11) and steady state parameters

the material necessary to fix the directors and reflector with the patch. The proposed design is shown in figure 3.16. An input impedance of 42.3 Ohms, which is closer to the 50 Ohms standard antenna input impedance is achieved, whereas the resonance frequency remained the same.

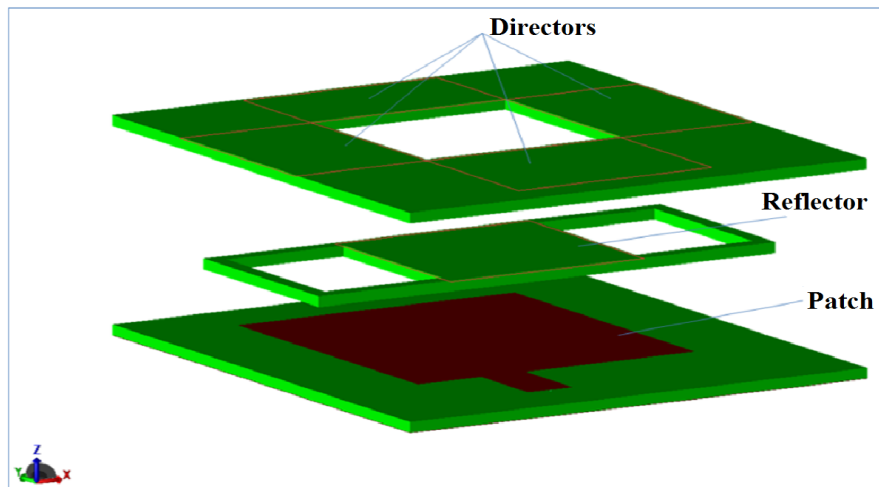


Figure 3.16: Microstrip patch antenna configuration with directors and reflector

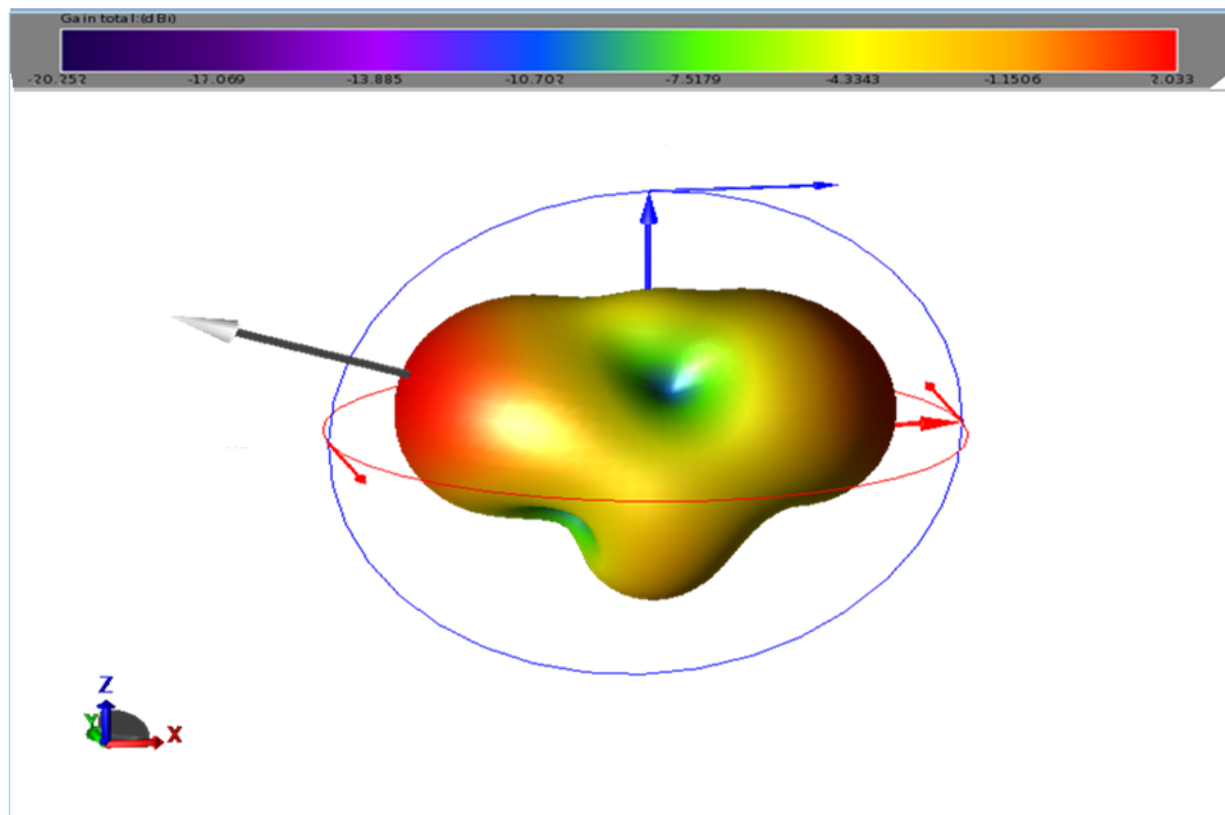


Figure 3.17: 3D far zone total gain

3.6 Design 2 : Loop Director and Rectangular Reflector

The configuration of the proposed microstrip patch is composed of one loop director and one rectangular reflector as shown in figure 3.18. It was observed from design 1 that the radiation pattern of the microstrip patch antenna is more uniform and horizontally directed when the four directors are placed close to each other. Based on this observation it was decided to replace the four directors with a loop to improve the radiation characteristics of the proposed antenna. The same substrate type and thickness was used for the loop director as the rectangular directors in design 1. The entire size of the designed structure is optimized as shown in table 3.2 in order to achieve a horizontal radiation with the highest possible gain.

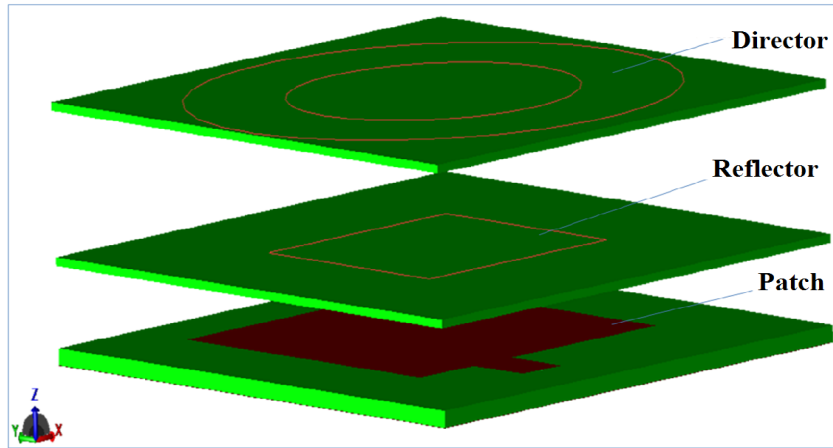


Figure 3.18: Microstrip patch antenna configuration with loop director

Director				Reflectors			
Outer Radius	Inner Radius	Location	Substrate (h)	Length	Width	Location	Substrate (h)
29.615 mm	17.5 mm	35 mm	0.794 mm	36.25 mm	36.25 mm	23 mm	0.794 mm
Total height = 35mm + 0.794mm =35.794 mm Dimensions = 61.875mm x 67.65mm x 35.794mm							

Table 3.2: Antenna Elements Dimensions, Locations, and Substrate Thickness

3.6.1 Radiation Pattern

Figures 3.19 and 3.20 present the 2D cut view and 3D far zone simulation result of the E-plane radiation pattern of the microstrip patch antenna configuration with a loop director. As shown in figure 3.19 a fully horizontal (0 degrees elevation) and symmetric radiation pattern is obtained, Also the vertical direction radiation was suppressed and made very low which helps to improve the overall performance of the

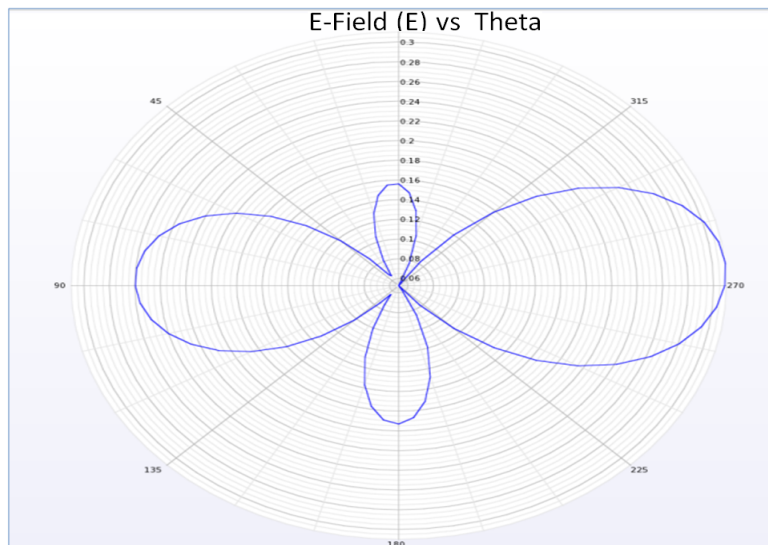


Figure 3.19: 2D ($\phi=0$ degrees) cut view of E- field

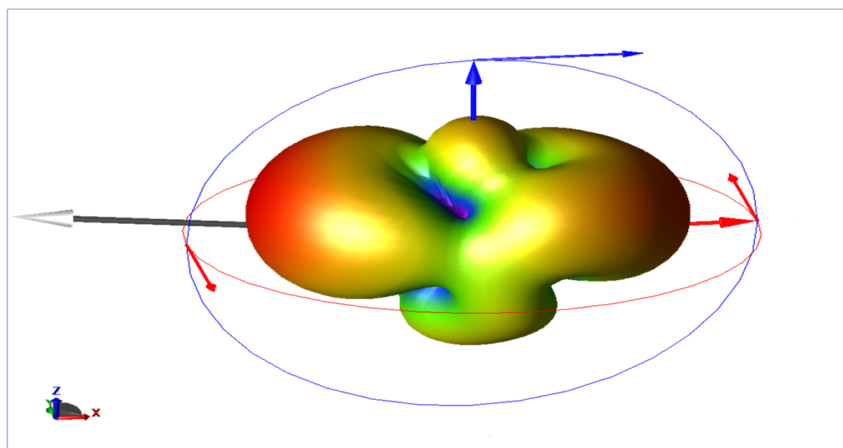


Figure 3.20: 3D far zone total E-Field distribution

3.6.2 Antenna Gain

The simulation results of the 2D cut view and 3D far zone gain for the microstrip patch antenna configuration with the loop director are presented in figures 3.21 and 3.22. A maximum gain of 1.972 dBi is obtained where the main lobe is directed to $\theta=90$ degrees and $\Phi=170$ degrees (0 degrees elevation). The gain is low because the microstrip patch antenna covers a wide solid angle which makes it best suited for applications that require a wide coverage in a short distance.

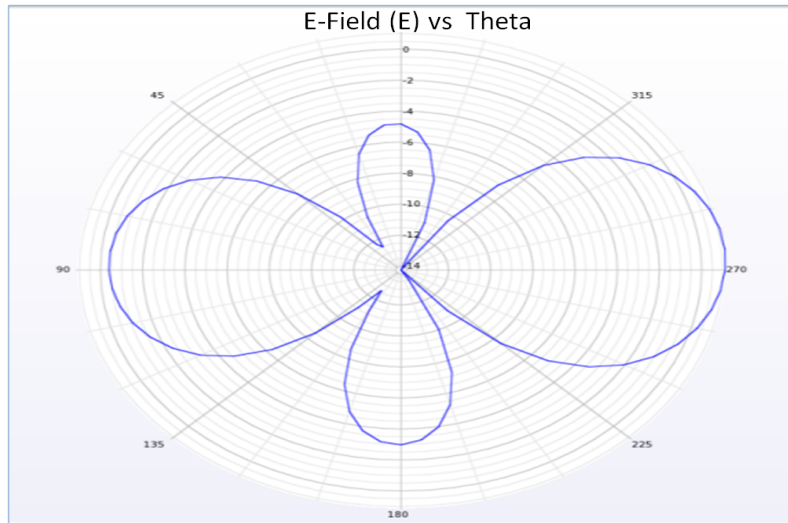


Figure 3.21: 2D ($\phi=0$ degrees) cut view of the gain

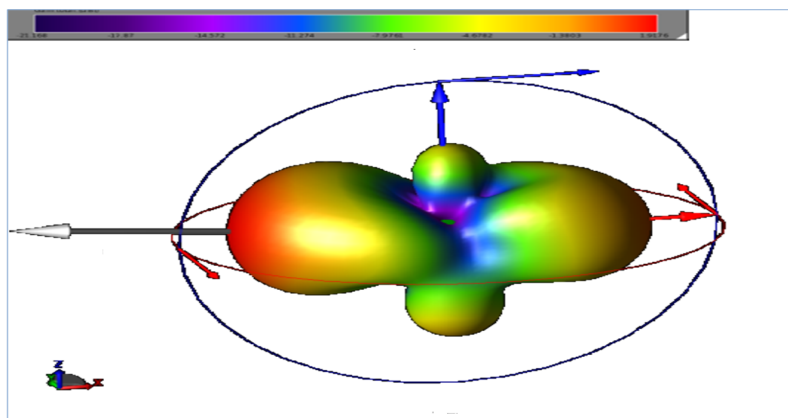


Figure 3.22: 3D far zone total gain

3.6.3 Return Loss

Figure 3.23 presents the S-parameter (S_{11}) and the time domain steady state parameters of proposed microstrip patch antenna configuration at 2.4GHz. It is observed that the resonant center frequency is close to the required resonant center frequency of 2.4GHz. An input impedance of 45.11 ohms is achieved which is within the range of 50 ohms for a standard antenna input impedance. A better return loss and antenna input impedance is achieved compared to design 1.

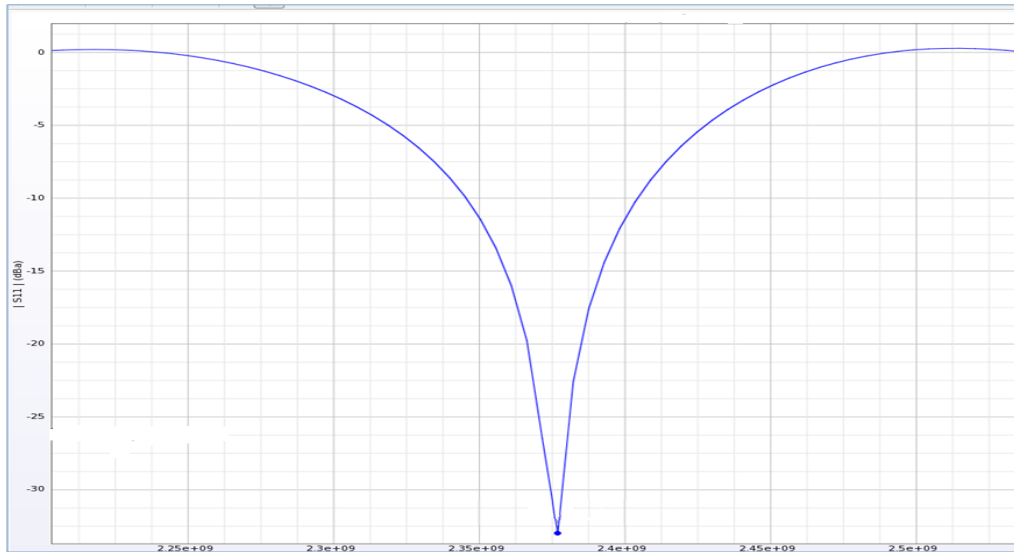


Figure 3.23: Return loss (S_{11}) and steady state parameters

In design 2 the proposed microstrip patch antenna configuration is made to radiate horizontally, resonant near the design frequency and acceptable input impedance is obtained. But the observed antenna gain is not very high. In order to improve the performance of the microstrip patch antenna configuration with a loop director, especially the gain, the reflector is modified in such a way to enhance the directivity of the microstrip patch antenna and reduce the solid angle of radiation as shown in figure 3.24. The optimized dimensions for the director and the reflectors and their respective positions are presented in table 3.3.

Figures 3.25 and 3.26 present the simulation result of the modified design, it can be seen that the gain of the microstrip patch antennas has been increased to 3.847 dBi in a horizontal direction ($\theta = 90$ degrees and $\Phi = 165$ degrees). Beside the gain

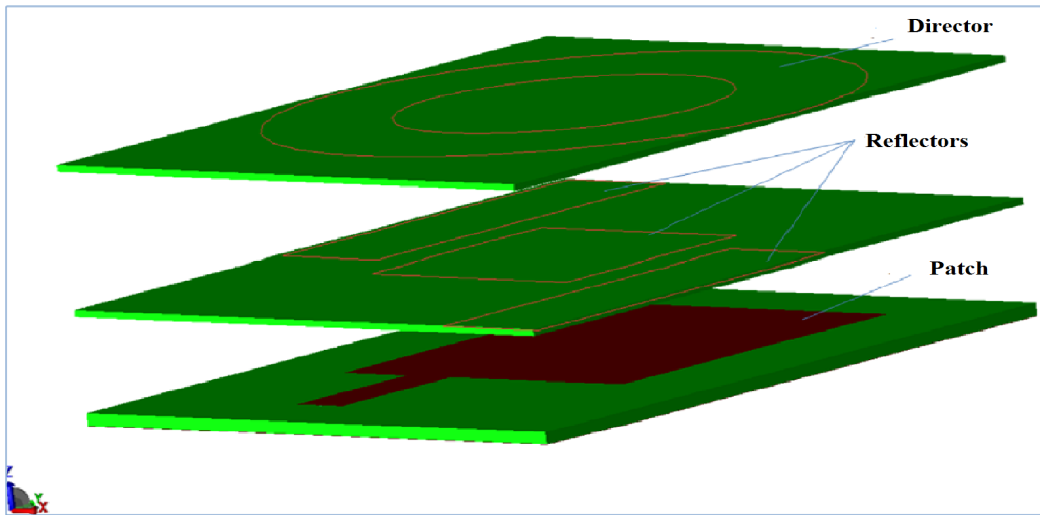


Figure 3.24: Microstrip antenna configuration with three reflectors

				Reflectors			
Director				Center reflector		Side reflector	
Outer Radius	Inner Radius	Location	Substrate (h)	Length	Width	Location	Substrate (h)
29.615 mm	17.5 mm	30 mm	0.794 mm	36.25 mm	36.25 mm	12.81 mm	44.35 mm
				Reflectors			
				Location		Substrate(h)	
				13 mm		0.794 mm	
Total height = 30mm + 0.794mm =30.794 mm Dimension = 61.875mm x 67.65mm x 30.794mm							

Table 3.3: Antenna Elements Dimensions, Locations, and Substrate Thickness

enhancement due to the added side reflectors the entire antenna structure height is reduced by 5 mm as shown in table 3.3. The resonant center frequency is also slightly shifted toward the design center frequency and an input impedance of 56.77 ohms is obtained as shown in figure 3.27.

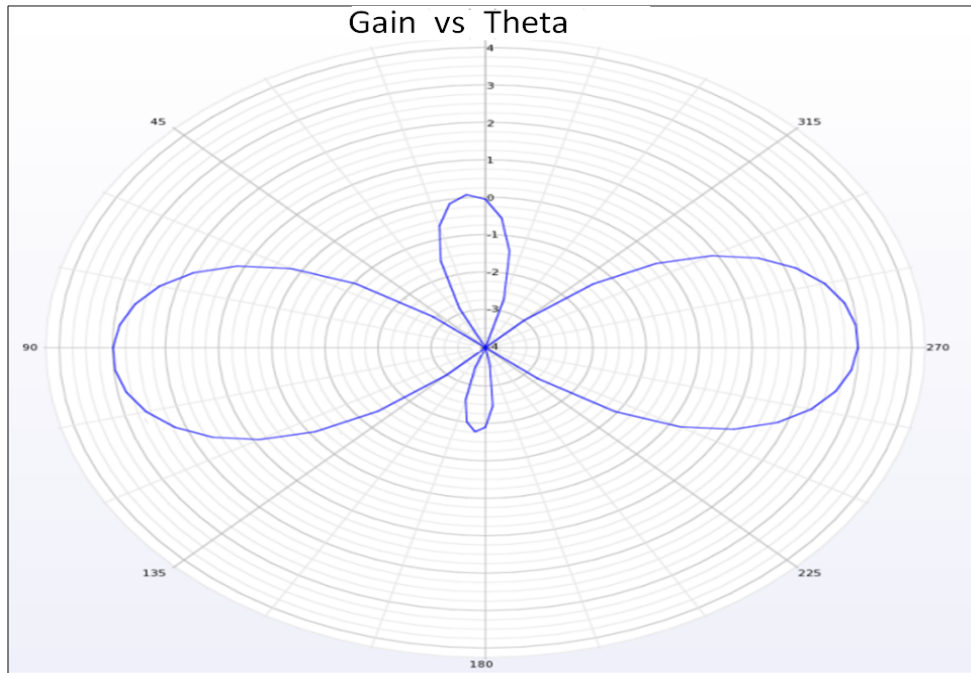


Figure 3.25: 2D ($\phi=0$ degrees) cut view of the gain

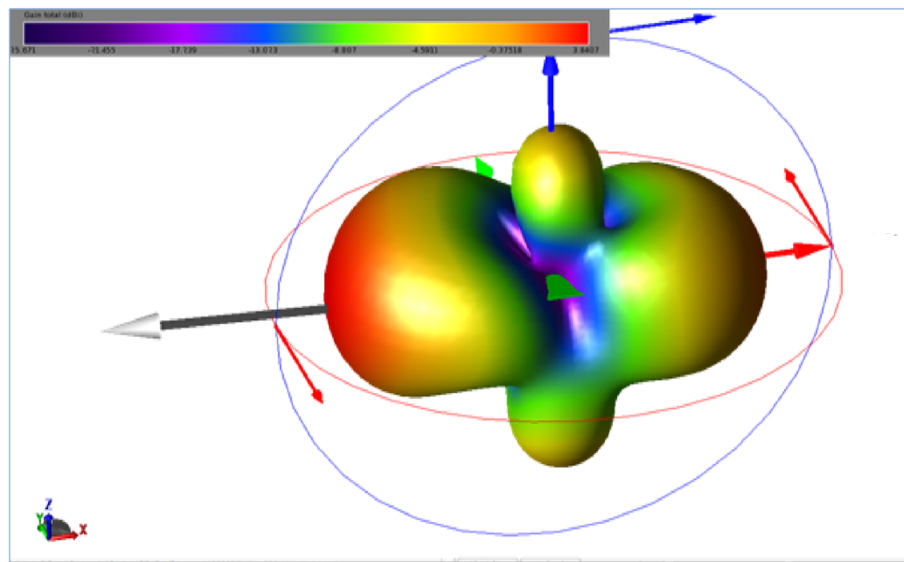


Figure 3.26: 3D far zone total gain

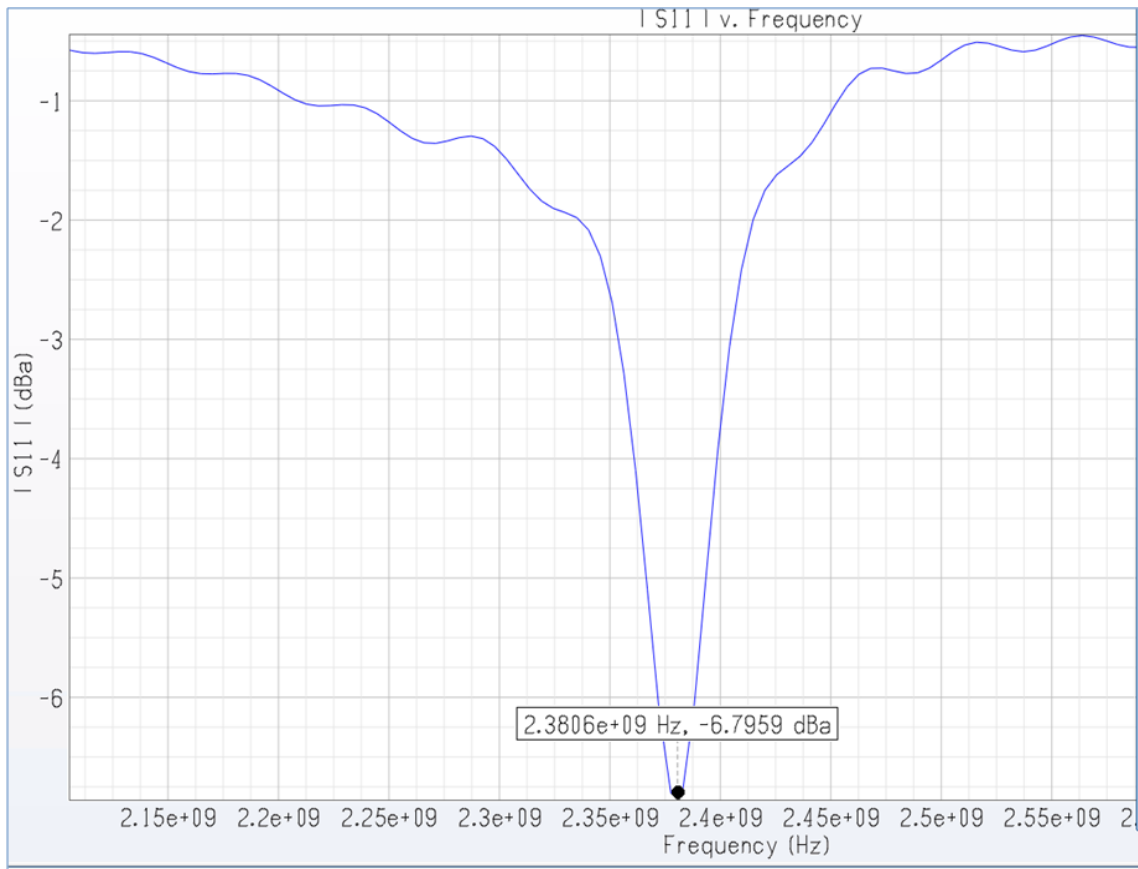


Figure 3.27: Return loss (S11) and steady state parameters

Chapter Four

Conclusion and Future Work

4.1 Conclusion

This research introduced and investigated a novel concept in the design of microstrip patch antennas with a radiation pattern in the horizontal direction. Two different antenna configurations with directors and reflectors to guide the radiated power in the horizontal direction were designed and simulated. The characteristics of the two proposed designs with respect to various parameters such as reflector dimensions, director dimensions, and spacing between these elements and the microstrip patch have been studied. The simulated results of the radiation pattern showed that the radiated power was horizontally directed on both designs which was insignificant for the standard microstrip patch antenna. The design with four rectangular directors and one rectangular reflector yielded a radiation pattern with an elevation of 20 degrees with a maximum gain of 2.033dBi. The proposed antenna structure has dimensions of 61.785mm x 67.65 mm and total height of 35.794mm. The overall size of the proposed antenna structure is compact compared to commercially available antenna of its type. The results from the design with one loop director and three rectangular reflectors yielded a radiation pattern with an elevation of 0 degrees with a maximum gain of 3.847 dBi. The compactness of the overall antenna structure was further improved to 61.875mm x 67.65mm and a total height of 30.794mm. The input impedance and resonance center frequencies for both designs were close to the calculated values according to the simulation results.

This work suggests that the proposed antennas configurations provide a light-weight, compact, low cost and better signal strength in horizontal direction compared to the regular microstrip patch antenna. These antennas present an excellent candidate for emerging wireless communications at 2.4 GHz frequency that require a transfer of

large amount of data in rapid bursts, which include Bluetooth and WiFi (802.11).

4.2 Future Work

The simulation results are good enough to justify fabrication of the proposed antennas on hardware to check the actual radiation performance. The investigation has been limited to theoretical studies and simulations due to lack of testing facilities at 2.4GHz frequency. In order to enhance the gain and other radiation performances of the antennas, additional directors/reflectors can be added accordingly. Using thicker substrates for those applications where the weight of the antenna is not an issue could improve the performance of the proposed designs. It is also expected that the size of the proposed antennas can be reduced approximately by half for 5GHz applications.

References

- [1] Constantine A. Balanis, "Antenna Theory: Analysis and Design, 3rd Edition," John Wiley and Sons, Inc. Hoboken, New Jersey 2005.
- [2] P. Bhartia , Inder Bahl , R. Garg, and A. Ittipiboon, "Microstrip Antenna Design Handbook," Artech House Inc. Norwood, MA 2001.
- [3] Jagdish. M. Rathod, and Y.P.Kosta, "Development of Feed for Parabolic Reflector Antenna," International Journal of Engineering and Technology, Vol. 1, No. 1, April, 2009, pp.1793-8236.
- [4] IEEE Standard Definitions of Terms for Antennas, Transactions on antennas and propagation, May 1969.
- [5] Edited by William A. Imbriale, Steven S. Gao and Luigi BocciaJohn, "Space Antenna Handbook," Wiley and Sons Ltd. West Sussex, UK 2012.
- [6] C.-C. Lin, L.-C. Kuo, and H.-R. Chuang, "A Horizontally Polarized Omnidirectional Printed Antenna for WLAN Applications," IEEE Transactions On Antennas And Propagation, Vol.54, No. 11, November 2006, pp.3551-3556.
- [7] "Antenna Fundamentals," <http://etd.lib.fsu.edu/theses/available/etd-04102004-143656/unrestricted/Chapter2.pdf>.
- [8] Dr. Steven R. Best, "Antenna Properties and their impact on Wireless System Performance," Cushcraft Corporation, Manchester, NH 03013.
- [9] Weili Ma, "Discrete Green's Function Formulation of the FDTD Method and its Application," Department of Electronic Engineering, Queen Mary University of London, United Kingdom, February 2004.
- [10] "EMPro 3D EM Simulation Software," <http://www.home.agilent.com/en/pc-1297143/empro-3d-em-simulation-software>.

- [11] Mouloud Challal¹, Arab Azrar¹ and Mokrane Dehmas, "Rectangular Patch Antenna Performances Improvement Employing Slotted Rectangular shaped for WLAN Applications," *IJCSI International Journal of Computer Science Issues*, Vol. 8, Issue 3, No. 1, May 2011, pp.254-258.
- [12] Shiv Kaushik Varanasi, "Investigations On Cavity Backed Wideband Microstrip Patch Antennas With Enhanced Performance For Wireless Communication Applications," San Diego State University, Fall 2010.
- [13] RongLin Li, Gerald DeJean, Moonkyun Maeng, Kyutae Lim, Stephane Pinel, Manos M. Tentzeris, and Joy Laskar, "Design of Compact Stacked-Patch Antennas in LTCC Multilayer Packaging Modules for Wireless Applications," *IEEE Transactions On Advanced Packaging*, Vol. 27, No. 4, November 2004, pp.581-589.
- [14] Olivier Kramer, Tarek Djerafi, and Ke Wu, "Vertically Multilayer-Stacked Yagi Antenna With Single and Dual Polarizations," *IEEE Transactions On Antennas And Propagation*, Vol. 58, No. 4, April 2010, pp.1022-1030.
- [15] John Huang, and Arthur C. Densmore, "Microstrip Yagi Array Antenna for Mobile Satellite Vehicle Application," *IEEE Transactions On Antennas And Propagation*, Vol. 39, No. 7, July 1991, pp.1024-1030.
- [16] ". RT/duroid-High Frequency Laminates," <http://www.rogerscorp.com/acm/products/10/RT-duroid-5870-5880-5880LZ-High-Frequency-Laminates.aspx>.
- [17] "Satellite Communications," <http://www.odysseyus.nildram.co.uk/>.
- [18] Gray A Thiele, "Analysis of Yagi-Uda-Type Antennas," *IEEE Transactions On Antennas And Propagation*, Vol. Ap-17, So. 1, January 1969, pp.24-31.
- [19] C.Soras, M.Karaboikis, G. Tsachtsiris and V. Markios, " Analysis and Design of an inverted-F antenna printed on a PCMCIA Card for 2.4GHz ISM Band," *IEEE Antenna's and Propagation Magazine*, Vol 44, No. 1, February 2002, pp.37-42.
- [20] J. E. RHODES Lieutenant General, U.S. Marine Commanding General Marine Corps Combat Development Command, "Antenna Handbook," Distribution: 144 000062 00.